

University of Montreal

**The Origin and Stimuli Implicated in the
Expression of Nestin⁽⁺⁾ Cardiac Myocyte-
like Cells in the Ischemic Heart**

By
John Assimakopoulos

Department of Physiology
Faculty of Medicine
University of Montreal

Memoir presented to the Faculty of Superior Studies
In light of obtaining the grade of
M.Sc. in Physiology

January 2009

©, John Assimakopoulos, 2009

University of Montreal
Faculty of Superior Studies

Memoir Title:

The Origin and Stimuli Implicated in the Expression
of Nestin⁽⁺⁾ Cardiac Myocyte-like Cells in the Ischemic Heart

Presented by: John Assimakopoulos

was evaluated by a jury composed of the following members:

Dr Angelino Calderone
Research Director

Dr Jocelyn Dupuis
President Reporter

Dr Madhu Anand-Srivastava
Jury Member

Abstract

Studies from our lab demonstrated that scar formation and healing was associated with the appearance of nestin⁽⁺⁾ cardiac myocyte-like cells predominantly at the peri-infarct region. The focus of the present study was to identify the underlying mechanism(s) (e.g. hypoxia, neurohormones) implicated in their recruitment and their cellular origin. The presence of these cells was detected as early as 1-week post-myocardial infarction (MI) and persisted 9 months after complete coronary artery ligation. Furthermore, nestin⁽⁺⁾ cardiac myocyte-like cells were also detected in the infarcted human heart. Hypoxia represents a predominant stimulus following MI, however the exposure of normal rats to a hypoxic environment failed to promote the re-appearance of nestin⁽⁺⁾ cardiac myocyte-like cells. By contrast, the infusion of the non-selective β -adrenergic agonist isoproterenol (ISO) in the normal adult Sprague-Dawley rat increased nestin expression in the left ventricle and was associated with the reappearance of nestin⁽⁺⁾ cardiac myocyte-like cells. However, the reappearance of nestin⁽⁺⁾ cardiac myocyte-like cells may not represent a direct effect but was apparently secondary to cardiac myocyte necrosis mediated by isoproterenol. Lastly, we identified a subpopulation of nestin-immunoreactive cells in the normal rat heart that co-expressed cardiac progenitor cell markers Nkx-2.5 and GATA-4. This subpopulation of nestin/Nkx-2.5/GATA-4 cells may represent the progenitor pool that differentiates to a nestin⁽⁺⁾ cardiac myocyte-like cell following an ischemic insult.

Key words: nestin, isoproterenol, cardiac myocyte, cardiac progenitor, necrosis

Résumé

Nos études ont démontrées que la formation de la cicatrice et la guérison sont associées avec l'apparition de cellules de type myocytes cardiaques nestine⁽⁺⁾ dans la région péri-infarctie. Présentement, l'étude examine le mécanisme, tel que l'hypoxie ou les hormones neuronales, possiblement impliqué dans leur recrutement et de dévoiler leur origine cellulaire. La présence de ces cellules a été détectée dans les coeurs infarcties d'une semaine et maintenue après neuf mois suite à une sujétion coronaire complète. Aussi, ces cellules de type myocytes cardiaques nestine⁽⁺⁾ ont été observées dans le coeur infarcté humain. L'hypoxie représente un événement prédominant suite à un infarctus de myocarde, mais l'exposition des rats normaux à un environnement hypoxique n'a pas pu promouvoir l'apparition de ces cellules. Autrement, l'infusion de l'agoniste β -adrénergique non-sélectif isoprotérénol (ISO) dans les rats adultes Sprague-Dawley a augmenté la protéine nestine dans le ventricule gauche et a été associé avec la réapparition de cellules de type myocytes cardiaques nestine⁽⁺⁾. Cela représente possiblement un effet secondaire suite à la nécrose des myocytes cardiaques par l'administration d'isoprotérénol. Dernièrement, on a identifié une sous-population de cellules nestine⁽⁺⁾ dans le coeur normal du rat qui co-exprime les marqueurs de cellules cardiaques progénitrices Nkx-2.5 et GATA-4. Cette sous-population de cellules nestine/Nkx-2.5/GATA-4 pourrait représenter des substrats cellulaires qui puissent se différencier en cellules de type myocytes cardiaques nestine⁽⁺⁾ suite à une ischémie.

Mots clés: nestine, isoprotérénol, nécrose, cellule souche, cellule progénitrice, myocyte cardiaque

Table of Contents

ABSTRACT	III
TABLE OF CONTENTS	VII
LIST OF FIGURES AND TABLES	VIII
LIST OF ABBREVIATIONS	XI
ACKNOWLEDGEMENTS	XV
INTRODUCTION	1
1. Prevalence of Myocardial Infarctions	2
1.1 Health Risks	2
1.2 Therapeutics	2
2. Myocardial Infarction	4
2.1 Coronary Occlusion	4
2.2 Reparative Fibrosis Post-MI	5
2.2.1 Role of Myofibroblasts	5
2.3 Post-MI Left Ventricular Remodelling	6
2.3.1 Hypertrophy	6
2.3.2 Reactive Fibrosis	7
2.4 Angiogenesis and Neurogenesis	7
2.5 Recruitment of Nestin ⁽⁺⁾ Neural Stem Cells	9
2.6 The Appearance of Nestin ⁽⁺⁾ Cardiac Myocyte-like Cells	11
2.7 Endogenous Cardiac Progenitor Stem Cell Pools	12
2.8 Neurohormones and Peptides Implicated in Post-MI Remodelling	13
3. Sympathetic Nervous System	14
3.1 Isoproterenol	14
3.2 Adrenergic Receptors	15
3.2.1 β_1 Adrenergic Receptors	17
3.2.2 β_1 Adrenergic Receptor Signalling	18
3.2.3 β_2 Adrenergic Receptors	24
3.2.4 β_2 Adrenergic Receptor Signalling	25
OBJECTIVES	27
MATERIALS AND METHODS	29
RESULTS	40
DISCUSSION	66
CONCLUSION	75
REFERENCES	77

LIST OF FIGURES AND TABLES

INTRODUCTION

- Figure 1: Myocardial infarction.
- Figure 2: Nestin⁽⁺⁾ neural stem cell.
- Figure 3: The structures of epinephrine and isoproterenol.
- Figure 4: The signalling pathways of the β -adrenergic receptors.
- Figure 5: Calcium regulation in muscular tissue.
- Figure 6: The structure of the sarcomere.
- Figure 7: The anti-apoptotic pathway of β_2 AR stimulation via the PI3K-Akt pathway.

RESULTS

- Figure 1: The absence of nestin-immunoreactive cardiac myocyte-like cells in the normal rat heart.
- Figure 2: The presence of nestin⁽⁺⁾ cardiac myocyte-like cells in 3-week post-MI adult rats.
- Figure 3: The presence of nestin⁽⁺⁾ cardiac myocyte-like cells in 9-month post-MI adult rats.
- Figure 4: Connexin-43 organization in the heart of sham and 1-week post-MI rats.

- Figure 5: The presence of nestin⁽⁺⁾/desmin⁽⁺⁾ cardiac myocyte-like cells in the infarcted human heart.
- Figure 6: The presence of nestin⁽⁺⁾ cardiac myocyte-like cells in the infarcted human heart.
- Figure 7: Nestin expression in the left and right ventricles of normoxic and hypoxic rats.
- Figure 8: Nestin⁽⁺⁾ cardiac myocyte-like cells undetected in the myocardium following hypoxia.
- Figure 9: Nestin immunoreactivity not detected in Cx43⁽⁺⁾ neonatal ventricular cardiac myocytes following both normoxic and hypoxic exposures
- Figure 10: Effect of hypoxic exposure on neonatal cardiac myocytes.
- Figure 11: Cardiac progenitor cell marker expression in normal adult rat hearts.
- Figure 12: Distinguished subpopulations of nestin and cardiac progenitor stem cells are intercalated in between cardiac myocytes in the normal heart.
- Figure 13: β_1 -adrenergic receptor (β_1 AR) immunoreactivity in nestin⁽⁺⁾ stem cells and nestin⁽⁺⁾ cardiac myocyte-like cells.
- Figure 14: Numerous nestin⁽⁺⁾ cardiac myocyte-like cells expressing β_1 -adrenergic receptors (β_1 ARs) in ISO-treated rats
- Figure 15: Smooth muscle α -actin, Bax, Bcl-2, and nestin expression in the left ventricle of sham and ISO-treated rats.
- Table 1: Body and heart weights of control and 1-week ISO-treated rats.
- Table 2: Hemodynamic parameters of control and 1-week ISO-treated rats.

- Figure 16: Quantitative analysis of protein expression in the left ventricle of sham and isoproterenol-treated rats.
- Figure 17: Sirius Red immunohistological staining of collagen in the left ventricle of sham and ISO-treated rats.
- Figure 18: Collagen mRNA expression in the left ventricle of sham and isoproterenol-treated rats.

LIST OF ABBREVIATIONS

α : Alpha

α AR: α -adrenergic receptors

AC: Adenylate cyclase

ACE: Angiotensin converting enzyme

ADP: Adenosine diphosphate

Akt: Protein kinase B

Ang II: Angiotensin II

Apaf-1: Apoptotic protease activating factor 1

ATP: Adenosine-5'-triphosphate

β : Beta

Bad: Bcl-2 associated death promoter protein

β AR: β -adrenergic receptor

Bax: Bcl-2 associated X protein

Bcl-2: B cell CLL/lymphoma 2

BDNF: Brain-derived neurotrophic factor

BSA: Bovine serum albumin

BW: Body weight

Ca²⁺: Calcium

CaMKII: Ca²⁺/calmodulin-dependent protein kinase II

cAMP: 3',5'-cyclic adenosine monophosphate

cDNA: complementary DNA

CO₂: Carbon dioxide

Cx43: Connexin-43

DABCO: 1,4-diazabicyclo[2.2.2]octane

DMEM: Dulbecco's Modified Eagle Medium

DMSO: Dimethyl sulfoxide

DNA: Deoxyribonucleic acid

ECL: Electrochemiluminescence

EDTA: Ethylene diamine tetraacetic acid

EGTA: Ethylene glycol tetraacetic acid

FBS: Fetal Bovine Serum

γ : Gamma

GAPDH: Glyceraldehyde 3-phosphate dehydrogenase

GATA-4: GATA-binding protein 4

GDP: Guanosine diphosphate

GPCR: G-protein coupled receptor

GTP: Guanosine triphosphate

H₂O: Water

HBSS: Hank's Balanced Salt Solution

HRE: Hypoxia response element

IgG: Immunoglobulin G

IP₃: 1,4,5-inositol triphosphate

ISO: Isoproterenol

ITS: Insulin transferase selenium

kDa: Kilo Dalton

LV: Left ventricle

LVEDP: Left ventricular end-diastolic pressure

LVSP: Left ventricular systolic pressure

MAPK: Mitogen-activated protein kinase

MEF-2C: muscle enhancement factor-2C

MI: Myocardial infarction

mRNA: Messenger ribonucleic acid

Na⁺: Sodium

NaF: Sodium fluoride

NF-M: Neurofilament-M

NGF: Nerve growth factor

NGS: Normal goat serum

NILV: Non-infarcted left ventricle

Nkx-2.5: NK2 transcription factor related, locus 5 (Drosophila)

O₂: Oxygen

PBS: Phosphate buffered saline

PCR: Polymerase chain reaction

PI3K: Phosphatidylinositol-3 kinase

PIP₂: Phosphatidylinositol 4,5-bisphosphate

PKA: Protein kinase A

PMSF: Phenylmethylsulphonyl fluoride

PVDF: Polyvinylidene fluoride

RNA: Ribonucleic Acid

RV: Right ventricle

Sca-1: Stem cell antigen-1

SDS: Sodium dodecyl sulfate

SBJ: Super blue juice

SERCA: Sarcoplasmic reticulum calcium-ATPase

SMA α : Smooth muscle α -actin

SR: Sarcoplasmic reticulum

TGF- β : Transforming growth factor beta

VEGF: Vascular endothelial growth factor

ACKNOWLEDGEMENTS

First and foremost, I would like to thank Dr Angelo Calderone for allowing me the opportunity to work in his laboratory. His vast knowledge and experience is one I aspire to reach coupled to his meticulous scientific analysis. Angelo's guidance has allowed me to develop as a future researcher and to be able to endure the long hard road that is ahead. He has taught me work efficiently, to look beyond what the results of an experiment show and how to appropriately apply the knowledge I have acquired. Over the past 2 years, his friendship has also provided me with a sense of belonging with our constant anecdotes before I would "get out of his office". Thank you Angelo for making me a part of your lab, your team, and most importantly, your friend.

Secondly, I would like thank my co-workers Hugues, Robert, Louis, Viviane, and Pauline. Their support and knowledge allowed me to grow as an individual and to realize that mixing up work with a little humor eases the mind. Viviane, your friendship and support has been greatly appreciated over the past 2 years, and our constant conversations have allowed me to fit in and become great friends. Pauline, your hard work ethic is quite admirable, and a trait I hope has rubbed off on me over the last year, because without you pushing me to work I would not have reached my goal today.

Finally, I would like to thank my family for the support, their belief in me, and their confidence that one day I would be achieve great things, and I am one step closer today to reaching that ultimate goal.

INTRODUCTION

1. Prevalence of Myocardial Infarctions

1.1 Health Risks

Environmental, genetic, and health risk factors can contribute to coronary artery disease ultimately leading to myocardial infarction (MI). The Heart and Stroke Foundation of Canada has reported that since 1994-95 there has been a steady rise in hospitalization due to heart attack with an estimated annual occurrence of 70 000 myocardial infarctions, with approximately 19 000 being fatal (Heart and Stroke Foundation of Canada, 2006). With 60% of Canadians being overweight or obese and nearly half of the population being inactive, the chances of diminishing heart attacks will be a constant uphill battle in the coming years and new tactics must be developed to overcome this rapidly emerging crisis (Heart and Stroke Foundation of Canada, 2004; Statistics Canada, 2007). Preventative measures can be undertaken by at-risk individuals as advised by their physician or by making personal lifestyle choices. In a similar fashion, modern medicine has its limitations to post-MI treatment via the administration of certain drugs as well as preventing damage at the onset of the MI. However, what if the heart possessed its own primitive repair mechanism to decrease the damage caused by this ever-growing pandemic. Stem cell research has constantly been addressing the unlimited potential that stem cells possess and how if cultivated within the proper conditions will be the future of medicine.

1.2 Therapeutics

Following a myocardial infarction, several therapeutic and pharmacological interventions exist that can limit further worsening of cardiac function and maladaptive remodelling. Nitroglycerin administration is a common prescription that has proven beneficial with its vasodilatory effect on the artery that was previously occluded. ACE inhibitors, such as captopril, aid in the treatment of post-MI patients via peripheral vasodilatation, ventricular unloading, and diminishment of ventricular hypertrophy (Sutton et al., 2000). β -blockers, including carvedilol, reduce the onset of post-MI remodelling events (Sutton et al., 2000).

However, what if the potential that lies in stem cells can be harvested, and conform them to the dire need at hand. Many researchers are evaluating whether stem cell cultivation is appropriate during gestation or at time of birth, and to store these cells aside for future use. Similarly, which type of drug administration can promote the differentiation of these cells into the desired cell type is still under intense research and evaluation. Undoubtedly, the prospective properties of these cells cannot be measured and have not fully been determined but still remain a key premise for discovery in times to come despite much ethical debate. This opens up a new realm of possibilities and new strategies for therapeutic treatments in post-MI patients.

2. Myocardial Infarction

2.1 Coronary Occlusion

A myocardial infarction occurs when the coronary artery is partially or fully occluded by an atherosclerotic plaque. The ensuing events will lead to left ventricular remodelling which is governed by several hormonal, genetic, and mechanical factors that will overlap and initiate pathophysiological changes in left ventricular morphology and function (Sutton et al., 2000).

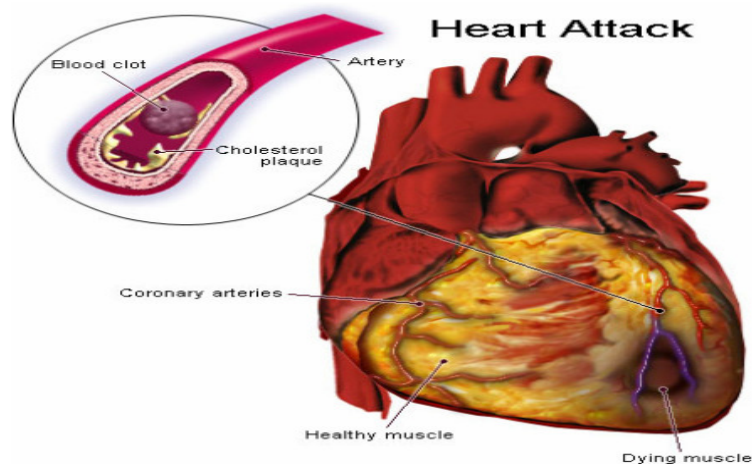


Fig. 1 - Myocardial infarction (http://www.straightfromthedoc.com/50226711/flickr_395241000.jpg).

The aftermath of the arterial occlusion coincides with a lack of oxygen supply creating a hypoxic environment in the afflicted cardiac area and the resulting death of the local myocyte population. In addition to the increase in diastolic load following an MI, many intracellular cascades will be activated and initiate pathophysiological changes ranging from left ventricular dilatation to the onset of collagen scar formation (Sutton et al., 2000). Similarly, the morphology, thickness,

and location of the scar will determine the amount of time that ventricular remodelling will require to counteract the distending forces with the scar's tensile strength (Sutton et al., 2000). Subsequently, the drop in pressure will be sensed by baroreceptors and lead to the release of angiotensin II (AII), which in turn will stimulate the production and secretion of catecholamines to increase inotropy and/or chronotropy in the heart via the sympathetic nervous system.

2.2 Reparative Fibrosis Post-MI

2.2.1 Role of Myofibroblasts

The infarct region refers to the hypoxic area where cellular necrosis has occurred and the necrotic cardiac myocyte population is replaced by granular tissue that will eventually undergo a cascade of physiological events leading to scar formation. The initial response consists of lymphocyte invasion to the ischemically damaged region. The subsequent release of inflammatory cytokines such as transforming growth factor- β (TGF- β) will promote the recruitment of cardiac fibroblasts from the non-infarcted left ventricle to the damaged area and initiate the differentiation to a myofibroblasts phenotype (Sutton et al., 2000). Myofibroblasts are characterized by the expression of smooth muscle α -actin and secrete higher levels of extracellular matrix proteins (e.g. fibronectin and collagen) to rapidly heal the ischemically damaged region via the formation of a permanent scar. This response represents an essential physiological mechanism required to heal the damaged heart as is denoted as reparative fibrosis.

2.3 Post-MI Left Ventricular Remodelling

2.3.1 Hypertrophy

Left ventricular remodelling is also separated into 2 stages, early and late remodelling. Early remodelling focuses on the expansion of the collagen scar while late remodelling revolves around the adaptations made by the infarcted portion of the left ventricle to compensate for the increase in wall stress (Sutton et al., 2000).

Cardiac fibroblasts are approximately 2/3 of the total cellular population of the heart, cardiac myocytes are the remaining 1/3 and occupy the majority of the area of the heart (Booz et al., 1995). Early remodelling refers to an early time frame post-MI where myocyte slippage leads to wall thinning and a reduction in the contractile area and volume of the left ventricle (Swynghedauw, 1999). In a study by Olivetti, 2 day post-MI rats had 63% myocytes slippage that led to a 20% increase in ventricular chamber dilatation, 33% decrease in wall thickness, and a 40% reduction in small calibre blood vessels in the scar (Olivetti et al., 1990). This subsequent increase in wall stress will potentiate the onset of cardiac hypertrophy and thus, late-stage remodelling.

In late remodelling, the pathophysiological and structural alterations occurring in the left ventricle due to myocyte death will serve to normalize the increase in systolic and diastolic wall stresses by acting as a potent stimulus for pathological eccentric cardiac hypertrophy (Sutton et al., 2000). In eccentric

cardiac hypertrophy, sarcomere genesis occurs in series leading to an increase in left ventricular chamber volume and is also characterized by a reversion to fetal gene expression affecting proteins such as the conversion of myosin α -heavy chain to the β -isoform and cardiac α -actin to the skeletal isoform (Schwartz et al., 1986). Similarly, there is a small concentric hypertrophic component occurring that will re-establish some slight wall thickness via parallel sarcomere genesis. Also, the onset of reparative fibrosis in the left ventricle will also help diminish the effects of high wall stress.

2.3.2 Reactive Fibrosis

In contrast, to the physiological response of reparative fibrosis, an increased deposition of collagen was also reported in the non-infarcted left ventricle (NILV) and is referred to as reactive fibrosis. The latter process is pathological and ultimately contributes to left ventricular dysfunction. Several studies support the premise that angiotensin II and the sympathetic system may synergistically promote cardiac fibroblast proliferation, thereby initiating the reactive fibrotic response.

2.4 Angiogenesis and Neurogenesis

In the ischemically damaged heart, the compensatory angiogenic response represents an integral event that attempts to prevent cardiac myocyte death in the ischemic region at risk thereby limiting infarct size. The intramyocardial injection of angiogenic peptides and administration of cellular substrates (e.g. endothelial

progenitor cells, bone marrow-derived cells) for *de novo* blood vessel formation have proven in part therapeutically efficient to limit infarct size. In addition to limiting size, angiogenesis contributes to scar thickening thereby ameliorating the healing process. It has been reported that an increase in scar thickness will limit infarct expansion and concomitantly reduce left ventricular dilatation, thereby improving left ventricular function (Lindsey et al., 2002; Wang et al., 2004).

It has been well established that myocardial infarction promotes sympathetic hyperinnervation, and the study by Vracko et al. (1990) was the first to report sympathetic fibers innervating the infarct region of the ischemically damaged rat heart. Subsequent studies by Drapeau et al. (2005) and El-Helou et al. (2005) confirmed these latter findings and an analogous paradigm was reported in the ischemically damaged human and dog heart as sympathetic fibers projecting from the left stellate ganglion were detected innervating the heart (Zhang et al., 2001; Zhou et al., 2004). Collectively, these data support the premise that sympathetic fiber sprouting and innervation of the damaged region represents a conserved event of myocardial healing across a wide range of species. The local release of nerve growth factor (NGF) by the ischemically damaged heart was identified as a possible candidate to promote sympathetic fiber sprouting (Matsuda et al., 1998).

During cutaneous and corneal wound healing, sympathetic fiber sprouting and innervation were reported and chemical sympathectomy was shown to impair the healing process (Kishimoto et al., 1982; Perez et al., 1987). The underlying

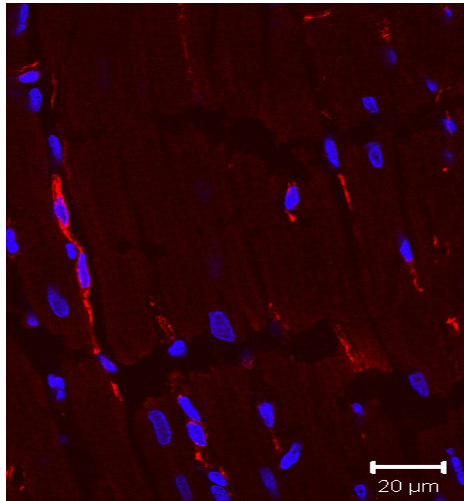
mechanism(s) attributed to the wound healing action of sympathetic fibers includes targeting invading myofibroblasts and angiogenesis. During cutaneous wound healing, nerve fibers were detected innervating myofibroblasts and the release of NGF was reported to promote myofibroblast proliferation and migration (Lui et al., 1999). Moreover, myofibroblasts represent an important source of NGF and acting via a paracrine mechanism promotes sympathetic fiber sprouting (Lui et al., 1999; Matsuda et al., 1998). Furthermore, their role in facilitating angiogenesis was identified because of the fact that sympathetic fiber denervation in skeletal muscle and brown adipose tissue reduced capillary density in response to cold exposure (Borisov et al., 2000; Asano et al., 1997). *De novo* blood vessel formation in the damaged tissue mediated by sympathetic fiber innervation may occur at least in part via the angiogenic action of brain-derived neurotrophic factor (BDNF) and NGF (Emanuelli et al., 2002; Donovan et al., 2000). Thus, sympathetic fiber innervation may play a seminal role in coordinating myofibroblast proliferation and angiogenesis to facilitate proper wound healing. In the ischemically damaged heart, data from Vracko et al. (1990), Drapeau et al. (2005), and El-Helou et al. (2005) suggests that the sympathetic system may play an analogous role.

2.5 Recruitment of Nestin⁽⁺⁾ Neural Stem Cells

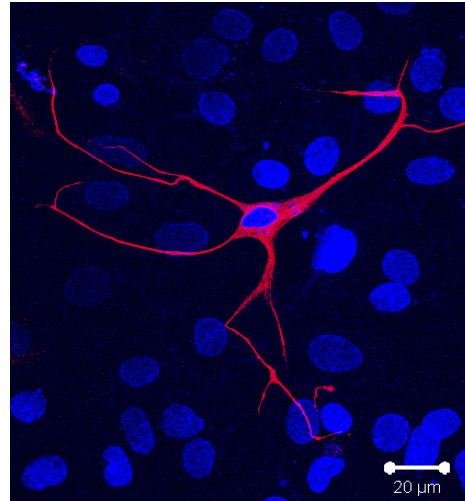
El-Helou et al. (2005, 2008) was the first to report that scar formation and healing was associated with the recruitment of a resident population of nestin-expressing neural crest-derived neural stem cells from the normal myocardium to

the ischemic region. Nestin is a type VI intermediate filament protein identified as a putative marker of neural stem cells and plays a role in various cellular functions including cell division and differentiation to axial growth in neurons (Michalczyk et al., 2005). In addition, transient nestin expression during embryonic development may serve as a temporary scaffold until replacement by tissue-specific intermediate filament proteins (Michalczyk et al., 2005). Similarly, the re-expression of nestin fibers following ischemic injury may further add to its speculative role in cell regeneration or remodeling (Michalczyk et al., 2005). Biologically, a subpopulation of neural stem cells isolated from the infarct region have the capacity to differentiate to either a vascular or endothelial cell, thereby representing a substrate for *de novo* blood vessel formation (El-Helou et al., 2008). Furthermore, during reparative fibrosis, nestin⁽⁺⁾ processes emanating from neural stem cells were detected innervating the peri-infarct/infarct region and physically associated with newly-formed neurofilament-M (NF-M) immunoreactive sympathetic fibers (El-Helou et al., 2005, 2008). These data suggest that an additional biological role of neural stem cells consists of promoting sympathetic fiber sprouting and subsequently guiding their innervation to the infarct region. These data are moreover clinically relevant as nestin-expressing cells characterized by a refractive cell body and numerous processes were also identified in the viable myocardium and infarct region of human patients and were morphologically identical to that observed in the rat heart (Fig. 2).

In Vivo Neural Stem Cells



In Vitro Neural Stem Cell

Fig. 2 - Nestin⁽⁺⁾ neural stem cell.

2.6 The Appearance of Nestin⁽⁺⁾ Cardiac Myocyte-like Cells

Unexpectedly, El-Helou et al. (2005) detected the presence of cardiac myocyte-like cells expressing the intermediate filament protein nestin, localized predominantly in the peri-infarct region. This observation was recently confirmed by the study of Scobioala et al. (2008), as nestin-immunoreactive cardiac myocyte-like cells were detected in the peri-infarct/infarct region of the ischemically damaged mouse heart. The findings are clinically relevant as the presence of numerous nestin-immunoreactive cardiac myocyte-like cells were also identified in the peri-infarct region of an infarcted human heart (El-Helou et al., 2008). Additional studies are required to address whether the appearance of these nestin-immunoreactive cardiac myocyte-like cells represents a transient response to an ischemic insult or is a permanent event associated with scar formation and healing

fibrosis. Furthermore, the stimulus implicated in their recruitment and the source of these cells remains undefined. The focus of the present thesis will address these aforementioned unresolved issues.

2.7 Endogenous Cardiac Progenitor Stem Cell Pools

Previous studies have already shown the multipotency of nestin-expressing stem cells by transdifferentiating into endothelial and neuronal phenotypes, thus resident nestin⁽⁺⁾ stem cell population are potential candidates in cardiac myocyte-like cell formation (Wurmser et al., 2004, Amoh et al., 2004, El-Helou et al., 2005). In addition to the nestin-immunoreactive neural stem cell population identified in the heart (Drapeau et al., 2005; El-Helou et al., 2005), other studies have demonstrated the presence of various cardiac progenitor stem cells, including GATA-4 and Nkx-2.5 cells, adding to the notion that the heart is not a terminally differentiated organ. Tomita et al. (2005) identified multipotent adult cardiac stem cells expressing stem cell antigen-1 (Sca-1) that are capable of differentiating into an endothelial and cardiac myocyte phenotype. Similarly, musashi-1 expressing neural crest-derived stem cells are present in the myocardium and can express the cardiac progenitor marker GATA-binding protein 4 (GATA-4) (Tomita et al., 2005). Muscle enhancement factor 2C (MEF-2C) represents another population of cardiac progenitor cells (Tomita et al., 2005). A small population of bone-derived c-kit⁽⁺⁾ (hematopoietic stem cell marker) stem cells have been identified in the myocardium and are capable of expressing Nkx-2.5 (Beltrami et al., 2003). It

remains to be determined if these cardiac progenitor cells or endogenous nestin⁽⁺⁾ neural stem cells are implicated in the formation of nestin-immunoreactive cardiac myocyte-like cells or other cellular phenotypes.

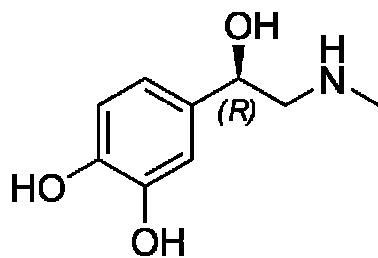
2.8 Neurohormones and Peptides Implicated in Post-MI Remodelling

Following an MI, many hemodynamic changes occur that can trigger intracellular cascades ranging from sympathetic nervous stimulation to the renin-angiotensin pathway (Sutton et al., 2000). The predominant physiological role of the sympathetic system following an ischemic insult is to provide inotropic and chronotropic support to the damaged heart. Moreover, the sympathetic system will recruit the renin-angiotensin-aldosterone system to maintain mean arterial blood pressure (Sutton et al., 2000). Furthermore, both the sympathetic system and angiotensin II participate in cardiac hypertrophy (Sutton et al., 2000) and their immediate recruitment following an ischemic insult may directly or indirectly contribute to the appearance of nestin-immunoreactive cardiac myocyte-like cells in the infarcted heart.

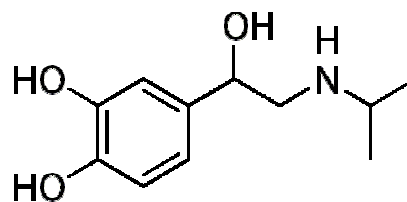
3. Sympathetic Nervous System

3.1 Isoproterenol

Isoproterenol, otherwise known as isoprenaline, is a synthetic sympathomimetic non-specific β_1 and β_2 receptor agonist with little affinity for α -adrenergic receptors (Voet et al. 2004). Its chemical structure consists of a benzene ring with multiple hydroxyl groups and an amino group, whose structure closely resembles that of the neurotransmitter and sympathetic agonist epinephrine (Fig. 3).



Epinephrine



Isoproterenol

Fig. 3 - The structures of epinephrine and isoproterenol.

Isoproterenol administration represents an established therapeutic approach to treat respiratory disease states such as asthma and bronchitis. In the heart, isoproterenol will act on β_1 and β_2 adrenergic receptors and elevate heart rate. It can exert inotropic and chronotropic effects such as elevated systolic blood pressure and vasodilatory effects including decreased diastolic blood pressure. Furthermore,

a high dosage of isoproterenol can create small pockets of necrosis within the myocardium or even induce myocardial infarction and arrhythmia.

3.2 Adrenergic Receptors

Adrenergic receptors interact with the autonomic nervous system and to its composite branches the sympathetic and parasympathetic nervous systems. These systems provide innervation to muscles and organs such as the adrenal glands and initiate biochemical processes that help us initiate the fight-or-flight action via the production of different endocrine hormones (Vander et al., 2001). All sympathetic pre-synaptic neurons will form a synapse with muscular motor end-plates (post-synaptic regions) known as the neuromuscular junction. Upon pre-synaptic membrane depolarization via action potential propagation and Na^+ entry, vesicles containing neurotransmitters will be released within the synapse (Vander et al., 2001). These neurohormones will then bind to specific receptors on the motor end-plates that will initiate Ca^{2+} entry within the muscle tissue, increase cytosolic Ca^{2+} levels, and commence the excitation-contraction process.

The cardiovascular system requires input from the sympathetic and parasympathetic nervous system to perform everyday functions. For example, they can influence pacemaker activity or ensure the necessary adaptations of heart rate, cardiac muscle contractility, systolic and diastolic pressures during moments of extreme stress, panic or exercise. Similarly, circulating catecholamines are able to

act on the heart via α - and β -adrenergic receptors (β ARs) and exert inotropic and/or lusitropic effects. The heart possesses more β ARs than α -adrenergic receptors (α ARs) (Vander et al. 2001).

β ARs are G-protein coupled receptors that contain conserved 7 hydrophobic transmembrane domains that anchor the receptor to the plasma membrane and have a cytoplasmic C-terminus and an extracellular N-terminus (Zheng et al., 2004). These receptors are coupled to trimeric G proteins involved in signal transduction. There are 2 subtypes of α ARs: α_1 and α_2 and there are 3 subtypes of β ARs: β_1 , β_2 , and β_3 . However, each of these receptor subtypes have functional variations in the cardiovascular system and differ in the signalling cascades they utilize to perform their physiological roles. The main focus will revolve around the β_1 and β_2 subtypes and their signalling pathways (Fig. 4).

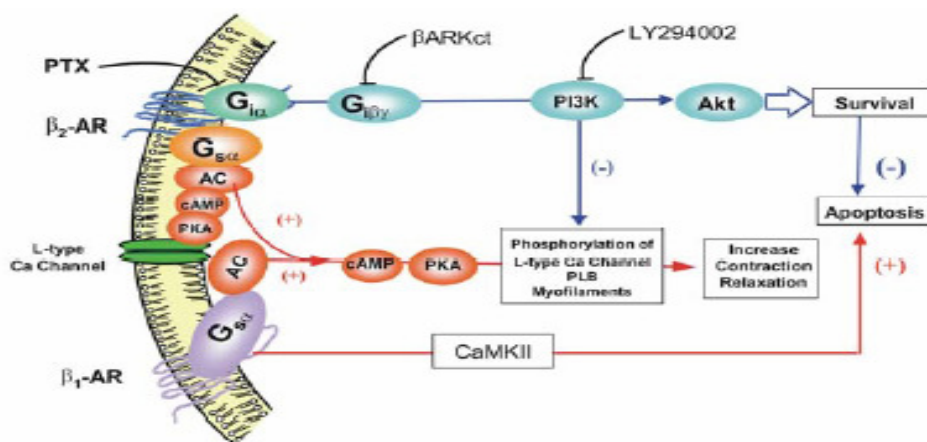


Fig. 4 - The signalling pathways of the β -adrenergic receptors (Zheng et al., 2004).

3.2.1 β_1 Adrenergic Receptors

The β_1 adrenergic receptor occupies 70-80% of the total β AR subtypes in the human ventricular myocardium (Brodde, 1991). It maintains 54% and 51% structural homology with the β_2 AR and β_3 AR respectively (Zheng et al., 2004). Its function in the heart serves to increase cardiac output by elevating heart rate via the depolarization of pacemaker cells in the sinoatrial node and heightened myocardial contractility in the left ventricle.

Studies on β_1 AR knockout mice revealed that when administered catecholamines, there were no remarkable variations in inotropy or heart rate suggesting the prevalent role of the β_1 receptor in cardiac regulation (Rohrer et al., 1996; Zheng et al., 2004). Clearly, this indicates how each β receptor subtype can constitute a different physiological and pathophysiological function from its cousin receptors.

In terms of functional role, the β_1 AR pathway can follow two distinct pathways; apoptosis and hypertrophy or contractility and relaxation.

3.2.2 β_1 Adrenergic Receptor Signalling

Contraction

The β_1 AR pathway works via $G_{s\alpha}$ -coupling. A guanosine triphosphate (GTP) molecule attaches to the receptor's α -subunit. In turn, this will cause a conformational change that will separate the α -subunit from the $\beta\gamma$ -subunit dimer, leading the α -subunit to activate adenylyl cyclase (AC) that will convert adenosine triphosphate (ATP) to cyclic adenosine monophosphate (cAMP) (Lodish et al., 2001). cAMP, acting as a second messenger, will activate protein kinase A (PKA) by separating the regulatory domain from the catalytic domain, and initiate a cascade of responses that will lead to increased inotropic and chronotropic effects. The intrinsic GTPase activity of the α -subunit, converting GTP to GDP, will then terminate the signal by dissociating from AC and re-binding to the $\beta\gamma$ -subunit dimer (Lodish et al. 2001).

Within the ventricular myocytes, the activated PKA will phosphorylate L-type Ca^{2+} channels on the sarcolemma (Zheng et al., 2004), leading to an influx of calcium into the myocytes from the T-tubules. The T-tubules contain vast reservoirs of calcium in sacs known as lateral sacs (Vander et al., 2001). Furthermore, phospholamban is inhibiting sarcoplasmic reticulum calcium-ATPase (SERCA) channels on the sarcoplasmic reticulum (SR) from re-absorbing the intracellular calcium. The high calcium levels inside the cell will again activate the ryanodine receptor (a Ca^{2+} -activated Ca^{2+} channel) on the SR and increase

cytoplasmic calcium levels. This rise in intracellular calcium levels will allow the sarcomere to contract and commence the heart's pumping action.

Similarly, the rise in intracellular Ca^{2+} levels can also be regulated by Ca^{2+} /calmodulin-dependent protein kinase II (CaMKII) independently of PKA (Zheng et al., 2004). Wang et al. (2004) provides evidence for this notion based on data obtained from inhibiting the PKA pathway and observing that it cannot fully impede the increase in Ca^{2+} as well as the contractile response. Concomitantly, blocking CaMKII activity can terminate sustained receptor stimulation (Wang et al., 2004). Furthermore, the data suggests that a time-dependent swap from the PKA pathway to CaMKII occurs based on tracing cAMP production and noting its desensitization following increased CaMKII activity (Hausdorff et al., 1990).

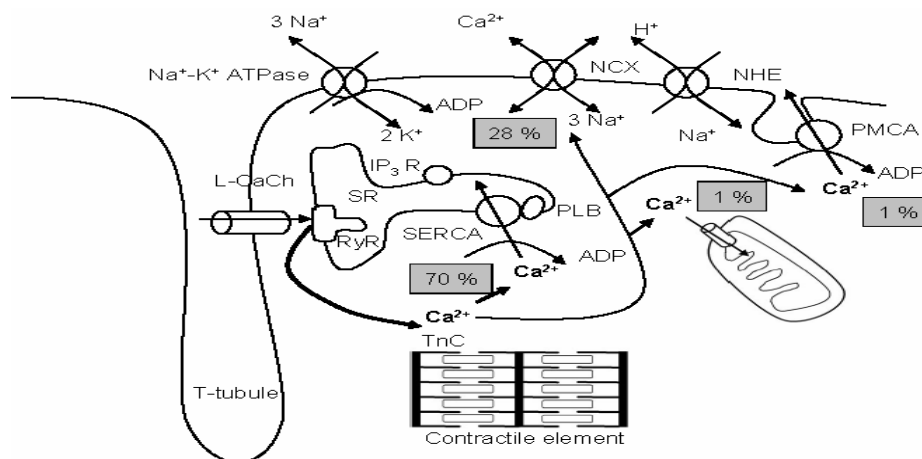


Fig. 5 - Calcium regulation in muscular tissue (<http://herkules.oulu.fi/isbn9514267214/html/graphic11.png>). This schematic is a representation of the Ca^{2+} channels implicated in calcium influx into the cytoplasm to initiate muscular contraction. It also displays the channels involved in the removal of calcium leading to muscular relaxation.

The Sarcomere: Muscular Contractile Unit

The cardiac muscle fibers, much like skeletal muscle, are basically comprised of several smaller fibers known as myofibrils. Each myofibril has contractile units known as sarcomeres whose organization allows for its organized striated appearance. Each sarcomere is comprised of thick filaments (myosin) and thin filaments (actin). Proteins such as titin and nebulin serve to stabilize and maintain the structure of the thick and thin filaments (Vander et al., 2001).

Each sarcomere is organized into several sections and delineations known as bands and lines (Fig. 5). Firstly there is the Z-line. The Z-line forms the border around each individual sarcomere and distinguishes it from its neighboring sarcomeres. It is where the thin filaments are anchored to the sarcomere at each end (Vander et al., 2001). The I-band refers to area in between the thick filaments of one sarcomere and the adjacent one. This area will decrease in size as the sarcomere contracts. The A-band is the area that myosin thick filaments occupy within the sarcomere. The H-band is the zone where the actin and myosin will interact with each other to reduce the length of the sarcomere and allow for muscular contraction to occur (Vander et al., 2001). Finally, the M-line is in the center of the H-band and delineates the center of the sarcomere where the coupling action between myosin's crossbridges and actin will occur (Vander et al., 2001).

The sliding-filament mechanism of the sarcomere will commence as soon as there is a calcium influx within the myocyte. The calcium will bind to troponin C

(a subunit of troponin) that will undergo a conformational change that will move tropomyosin with the aid of troponin T (Lodish et al., 2001). Tropomyosin blocks the myosin sites on the actin filaments to prevent maintained contractions. Similarly, molecules such as PKA, mentioned earlier, will also remove the troponin I inhibitory effect on troponin. An ATP molecule will bind to the myosin head and hydrolyze into ADP that will allow it to bind to actin and initiate the sliding movement of thick filament over thin filament. This will cause a shortening of the sarcomere unit and muscular contraction to occur. Once a new ATP molecule binds to the myosin it will detach from actin and begin the process anew (Vander et al., 2001).

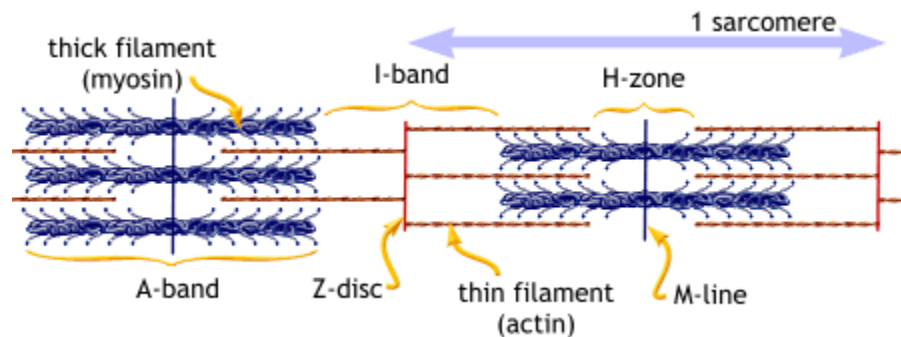


Fig. 6 - [The structure of the sarcomere \(http://www.blobs.org/science/cells/sarcomere2.gif\)](http://www.blobs.org/science/cells/sarcomere2.gif).

Relaxation

Muscular relaxation is simply the removal of the high levels of intracellular calcium within the myocyte by the activation of sarcolemmal and SR channels. Once an inhibitory agonist binds to the receptor or the GTP molecule is hydrolyzed,

it will lead to the eventual re-association of the α -subunit with the $\beta\gamma$ -subunit and terminate the activity of adenylyl cyclase. Sodium-calcium exchangers and calmodulin-dependent Ca^{2+} ATPase on the sarcolemma allow for calcium to exit the cell. Calcium re-enters the T-tubules and calcium is re-stored in the lateral sacs. Cytosolic calcium can exit also via mitochondrial Ca^{2+} channels. Similarly, phosphorylation of phospholamban by PKA removes its inhibition on SERCA allowing for Ca^{2+} re-entry into the SR.

Also, the second messenger can be adversely affected to terminate the contractile response. Phosphodiesterases serve to degrade cAMP to 5'-adenosine monophosphate (5'-AMP) and halt the activation of PKA's catalytic domain (Lodish et al., 2001).

The end result is that low levels of Ca^{2+} will impede troponin's conformational change that allows the subsequent binding of the myosin head to actin and thus, allow for sarcomeric length increase and relaxation.

Apoptosis

In addition, to the contraction-relaxation effects of adrenergic signalling, β_1 adrenergic stimulation is known to cause apoptosis. Previous studies have discussed the possibility that the cAMP/PKA pathway to be linked to programmed cell death (Communal et al., 1998; Iwai-Kanai et al., 1999). Different types of adenylyl cyclase have been overexpressed to observe their potential effects with

regards to apoptosis. Overexpression of type V and type VI adenylate cyclase do not corroborate with an increase in apoptotic levels but increased PKA activity (Tepe et al., 1999) and increased cardiac contractility (Gao et al., 1999). However, recently the rise in cytoplasmic calcium level that is coupled with an increase in myocardial contractility was in fact due to CaMKII and not linked to the PKA pathway (Zheng et al., 2004). CaMKII blockers significantly reduce the onset of apoptosis following β_1 receptor signalling versus using blockers for PKA (Zhu et al., 2003). Thus, the activity of CaMKII leads to intracellular Ca^{2+} overload and an eventual increased wear and tear on the myocytes and subsequent cellular death.

During apoptosis, pro-apoptotic proteins such as Bax are activated that will bind to the mitochondrial membrane of the cardiac myocyte. These pro-apoptotic factors will polymerize together to form pores or associate with the permeability pore complex for subsequent permeabilization of the outer mitochondrial membrane. In contrast, other pro-apoptotic proteins, such as Bad, will bind and inhibit anti-apoptotic proteins, such as Bcl-2, from ensuring caspase activation via Apaf-1 blockade (Lodish et al., 2001). Consequently, the ensuing event will result in apoptotic factor release from the mitochondria, including cytochrome c, that will bind to Apaf-1 leading to the formation of the apoptosome and in turn activate the proteolytic enzymes of the caspase family (Lodish et al., 2001).

Hypertrophy

β AR stimulation is capable of inducing ventricular hypertrophy. Following isoproterenol administration, the chronic activation of the β ARs leads to the upregulation of β -adrenergic receptor kinase-1, which phosphorylates and leads to the membrane downregulation of β ARs (Iaccarino et al., 1999). The subsequent impairment of β -adrenergic receptor activity may lead to a compensatory ventricular hypertrophic response during pressure overload by which the mechanism to induce hypertrophy remains unknown (Iaccarino et al., 1999).

3.2.3 β_2 Adrenergic Receptors

The β_2 adrenergic receptor occupies about 20-30% of the total β AR subtypes in the human ventricular myocardium (Brodde, 1991). It maintains 54% and 46% structural homology with the β_1 AR and β_3 AR respectively (Zheng et al., 2004). Its physiological functions are identical to that of the β_1 receptor but to a lesser degree of intensity most likely due to its lower density presence in the myocardium. Evidence for this is shown in β_2 AR knockout mice following catecholamine administration and how a complete cardiac response is elicited (Zheng et al., 2004). Similarly, β_1 AR knockout mice display a lack of this heightened response demonstrating how they are not the primary receptors for inotropic and chronotropic reactions (Rohrer, et al. 1996; Zheng et al., 2004).

3.2.4 β_2 Adrenergic Receptor Signalling

Contraction, Relaxation, and Anti-Apoptosis

Unlike β_1 ARs that have G_s signalling, β_2 ARs have dual coupling to G_s and G_i (Zheng et al., 2004). The associated G_i signalling provides a cardioprotective effect by reducing the dramatic results of G_s stimulation and promoting cell survival (Zheng et al., 2004). For instance, β_2 AR G_i signalling activates the $\text{Na}^+/\text{Ca}^{2+}$ exchanger on the sarcolemma leading to Ca^{2+} unloading in the sarcoplasmic reticulum (Sato et al., 2004). However, it exerts its anti-apoptotic effects by coupling to the PI3K-Akt pathway and not through MAPKs (Chesley et al., 2000; Zheng et al., 2004).

The G_s signalling remains identical to β_1 AR via the classic adenylyl cyclase-cAMP-PKA pathway leading to a subsequent rise in intracellular Ca^{2+} levels, though not as elevated as through β_1 AR regulation to induce myocardial contraction. The relaxation signalling process remains the same as that for β_1 AR.

The anti-apoptotic effects of β_2 stimulation are G_i -dependent following in vitro β_2 AR blocking (Communal et al., 1999). The cardioprotective G_i pathway commences with the activation of phosphatidylinositol-3-kinase (PI3K) (Fig 6). Whether it is $G_{i\alpha}$ - or $G_{i\beta\gamma}$ -coupled, it remains unclear. PI3K will in turn phosphorylate phosphatidylinositol-2-phosphate (PIP_2) and convert it to phosphatidylinositol-3-phosphate (PIP_3). PIP_3 activates Akt (or protein kinase B)

via phosphorylation, which will phosphorylate and inactivate apoptotic factors such as Bad and ensure cell survival (Chang et al., 2003). Inhibiting the G_i -PI3K-Akt pathway results in β_2 AR stimulation switching to promote apoptosis (Zhu et al., 2001).

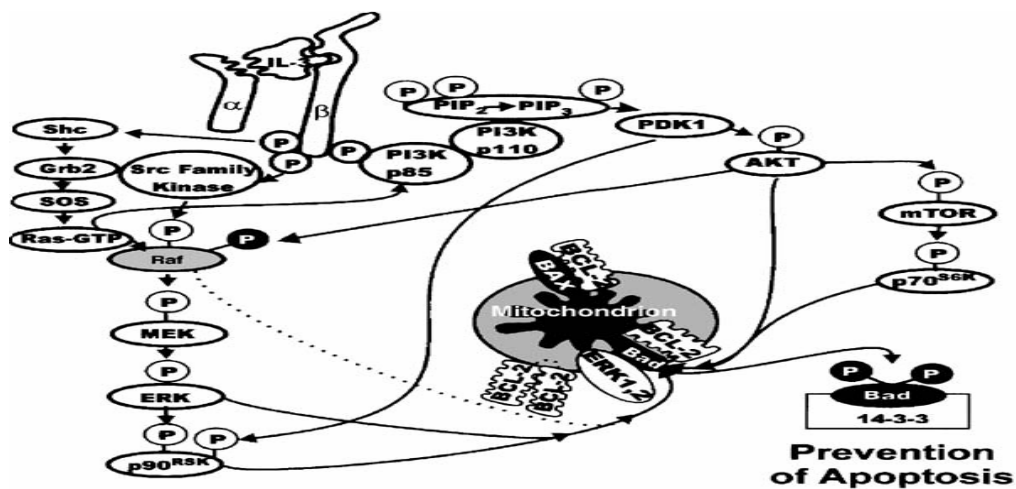


Fig. 7 - The anti-apoptotic pathway of β_2 AR stimulation via the PI3K-Akt pathway (Chang et al., 2003).

OBJECTIVES

Scar formation and healing is essential to heal the ischemically damaged heart and involves the interplay of numerous physiological events including inflammation, myofibroblast deposition of collagen, angiogenesis, and sympathetic fiber innervation mediated by cardiac neural stem cells. Work from Calderone's group revealed the novel observation that following ischemic injury to the rat, the peri-infarct/infarct region contained an abundance of nestin-immunoreactive cardiac myocyte-like cells (El-Helou et al., 2005, 2008). An analogous paradigm was reported in the infarcted human heart. Thus, the primary objective of the present thesis is to identify the phenotype and origin of nestin-immunoreactive cardiac myocyte-like cells and the stimuli implicated in the expression.

MATERIALS AND METHODS

Experimental Models

Human MI Tissue

The use of human cardiac tissue was approved by the Clinical Ethics board of the Montreal Heart Institute. Cardiac tissue samples (non-infarcted left ventricle and infarct region) were obtained from patients (3 males, 1 female; range 30-83 years old) who died either 1 week (n = 2) or 3 months (n = 2) following myocardial infarction. These samples were previously used in the study by El-Helou et al. (2008).

MI Rat Model

In this experimental model, we are creating a myocardial infarction in the rat by ligating the left anterior descending coronary artery and then allowing the rat to survive for a specific period of time post-MI ranging from 1 week to 9 months. Male Sprague Dawley rats (Charles River) weighing approximately 200-250 g were under initial anaesthesia using 3% isoflurane, followed by a reduction to 1.5% during the ligating procedure. Following the post-MI survival period, the hearts were excised and stored in either 2-methylbutane to perform immunofluorescence, frozen in liquid nitrogen for use in molecular biology experimentation, or in formalin for immunohistochemistry. The use and care of laboratory animals was according to the Canadian Council for Animal Care and all animal studies were approved by the Animal Care Ethics Committee of the Montreal Heart Institute.

Hypoxia Rat Model

Male Sprague-Dawley rats (200-250 g; Charles River) were placed in a Plexiglas chamber (width 63 cm; height 43 cm; depth 60 cm) into which a continuous flow of air and pure nitrogen mixture was delivered, resulting in an inspired oxygen fraction (FiO_2) of 0.12. The flow rates of the gases were controlled using individual flow meters, and the FiO_2 was confirmed using an oxygen analyzer (Applied Electrochemistry model S-3A/I). Exposure to continuous hypoxia was maintained for 10 days and then the rats immediately sacrificed. The sham rats were maintained in ambient air. The hearts of all animals were subsequently stored in 2-methylbutane.

Isoproterenol Infusion Rat Model

Male Sprague-Dawley rats (200-250 g; Charles River) were implanted (intraperitoneally) with osmotic pumps (model 2ML1, 10 μ L/hr; Alzet) containing either isoproterenol (infusion rate; 30 mg/kg/day) or saline for a period of 1 week. Rats were subsequently sacrificed, the hearts excised and stored in either 2-methylbutane to perform immunofluorescence or frozen in liquid nitrogen for protein/mRNA experiments.

Hemodynamic Measurements

The rats were anaesthetized using a mixture of ketamine (50 mg/kg) and xylazine (10 mg/kg). The lead electrodes were inserted in the left and right arms, and the left leg to measure and establish Einthoven's triangle to provide the electrocardiogram to view the electrical activity of the heart. The EMKA 1.8.11.12 program also provided a measure of the heart rate by the addition of the QR or measuring the systolic pressure curves.

Carotid catheter insertion method was used to measure the arterial pressure and the left ventricular pressure. Similarly, a jugular catheter insertion measured the right ventricular pressure. The method also calculated the rate of contraction (dP/dT), based on the steepest point of the ascending pressure curve, and the rate of relaxation based on the steepest point of the descending pressure curve. The diastolic pressure is represented by the smallest pressure reading of the pressure curve. The end-diastolic pressure is the point when the slope begins to rise and the systolic pressure is the highest peak point of the curve.

Cultured Neonatal Rat Cardiac Myocytes and Exposure to Hypoxia

Hearts were removed from 1-3 day old neonatal Sprague-Dawley rats anesthetized with ether and killed by decapitation. Ventricular tissues were placed immediately in chilled Ca^{2+} -free HBSS (GIBCO) and digested with 0.1% trypsin (GIBCO) in HBSS overnight at 4 °C. Ventricular cells were subsequently recovered by repeated digestions in 10 mL of 0.1% collagenase type II (GIBCO). The supernatants collected from each digestion were centrifuged and re-suspended in ice cold HBSS, followed by another centrifugation and re-suspension in DMEM containing 7% heat-inactivated FBS (GIBCO). The cells were preplated twice in T75 flasks (VWR) to enrich for myocytes and decrease contamination by nonmuscle cells. The non-adherent myocytes were then plated (100 mm plate; VWR) at a density of 100-200 cells per mm^2 for protein and mRNA studies. After 24 hours, the culture medium was changed to serum-free DMEM containing ITS (5 $\mu\text{g}/\text{ml}$ insulin, 5 $\mu\text{g}/\text{ml}$ transferrin, 5 ng/mL sodium selenite; GIBCO); all experiments were performed 24 hours later.

Neonatal rat ventricular myocytes were placed in a humidified chamber (In Vivo 400 Work Stations) maintained at 37 °C. An oxygen sensor constantly monitored the atmosphere and ensured hypoxic conditions by maintaining the oxygen level at 1%. Myocytes were exposed to a hypoxic environment for either 8 or 24 hour periods and nestin protein and mRNA levels were assessed. As a positive control, VEGF mRNA expression was determined. The normoxic environment consisted of 5% CO_2 and 21% O_2 at 37 °C.

Biochemistry Techniques

Protein Extraction

Cardiac tissue or cell cultures were lysed in a buffer containing 10 mM Tris (pH 7.5), 150 mM NaCl, 1 mM EDTA, 1 mM EGTA, 50 mM NaF, 0.5 mM PMSF (0.174 g/10 mL in ethanol), 1 mM sodium vanadate, 1% Triton X-100, 0.5% Igepal CA-630, 1 µg/mL of aprotinin (1 mg/mL in H₂O), and 1 µg/mL of leupeptin (1 mg/mL in DMSO). The tissue sample was placed in a 50 mL tube containing 2-3 mL of the lysis buffer. The tissue was grinded using the Polytron and the samples settled on ice for 1 hour. The homogenate samples were centrifuged at 10 000 RPM for 10 minutes at 4 °C. The supernatant was collected and stored at -20 °C. The protein concentration was measured using the Bradford assay technique.

Western Mini-Gel Electrophoresis, Transfer, and Blot

The results from the Bradford assay technique were used to calculate and load a protein sample 100 µg in weight. Acetone precipitation concentrated low concentration lysates into pellets followed by dissolution in 10 µL SBJ 1X. Concentrated samples were directly mixed with SBJ 2X for 25 µL loading volume. The SBJ contained 1 M Tris (pH 6.8), 30% glycerol, 6% SDS, 15% β-mercaptoethanol, and bromophenol blue. Prior to loading, the samples were then heated at 70 °C for 1-2 minutes to allow protein denaturation.

The lysates were subjected to SDS-polyacrylamide gel (10-15%) electrophoresis and protein subsequently transferred to a PVDF membrane. Immunoblotting was performed using 5% skim milk or BSA for 1-2 hours followed by successive PBS-Tween washings. The primary antibody was added and incubated at 4 °C overnight. The antibodies employed include mouse monoclonal anti-nestin (1:500; Millipore), mouse monoclonal anti-GAPDH (1:1000000; Ambion), mouse monoclonal anti-smooth muscle α -actin (1:2000; Sigma), mouse monoclonal anti-Bax and anti-Bcl-2 (1:500; Santa Cruz Biotechnology). Following overnight incubation at 4 °C, goat anti-mouse conjugated to horseradish peroxidase (1:10000, Santa Cruz Biotechnology) was added and visualization of the bands were detected by autoradiography utilizing the ECL detection kit (PerkinElmer Life Science).

Immunofluorescence

The rat heart was excised, immediately immersed in 2-methylbutane and stored at -80 °C. Primary passage neonatal rat ventricular myocytes were fixed with 4% paraformaldehyde prior to staining. Tissues were sectioned at 14 μ m using the cryostat and placed on poly-lysine coated slides and fixed with 4% paraformaldehyde (pH 7.2). Fixed cells or tissue were permeabilized with 2% normal goat serum (NGS) and 0.5% Triton X-100 for 1-2 hours at room temperature, and subsequently incubated overnight at 4°C with the appropriate antibody diluted in 1% NGS and 0.1% Triton X-100. Antibodies employed include mouse monoclonal anti-nestin (1:500; Millipore), rabbit polyclonal anti-desmin

(1:600; Abcam), rabbit polyclonal anti-NFM (1:500; Millipore) rabbit polyclonal anti- β_1 -adrenergic receptor, anti-Nkx-2.5, anti-GATA-4, and anti-connexin-43 (Santa Cruz Biotechnology). Following incubation, fixed tissue or cells were incubated for 1-2 hours at room temperature with either goat anti-mouse IgG conjugated to Alexa Fluor 555 (1:600; Invitrogen; emission wavelength at 570 nm) or goat anti-rabbit IgG conjugated to Alexa Fluor 488 (1:800; Invitrogen; emission wavelength at 520 nm) diluted in 0.05-0.1% Triton X-100 in PBS containing 1% NGS. To stain the nucleus, cells or tissue were initially treated with RNase (100 $\mu\text{g}/\mu\text{L}$; MBI Fermentas) for 20 minutes at 37 °C and then incubated for 20 minutes at room temperature with the fluorescent label to-pro³ (Invitrogen; 1.5 μM ; emission wavelength 661 nm). Non-specific staining was determined following the addition of either an isotype control antibody (mouse IgG, 5 $\mu\text{g}/\text{mL}$; rabbit IgG, 17 $\mu\text{g}/\text{mL}$) or the secondary antibody alone. The concentration of each isotype control was equivalent to the highest concentration of antibody employed. The slides were mounted on a 1:4 mixture of DABCO and glycerol prior to confocal microscope visualization. Immunofluorescence staining was visualized with either 10X- or 63X-oil 1.4 NA DIC plan apochromat objective mounted on a Zeiss Axiovert 100M confocal microscope.

Molecular Biology Techniques

Real-Time Polymerase Chain Reaction (Real Time-PCR)

Total RNA was isolated from the control and treated samples of cell cultures and/or ISO-treated adult rat hearts by a modification of the guanidine isothiocyanate-phenol-chloroform method. A cDNA library was generated by incubating 5 ng/ μ L total RNA (each sample), M-MLV reverse transcriptase (800 U, Invitrogen), RNaseOUT (40 U, Invitrogen), random-hexamer primers (0.04 U, Amersham Biosciences), dNTPs (0.5 mmol/L, MBI Fermentas), and supplied optimal buffers. The reaction protocol consisted of 3 successive incubation steps at (1) 25 °C for 10 minutes, (2) 37 °C for 50 minutes, and (3) 70 °C for 15 minutes.

Real-time polymerase chain reaction (PCR) was performed on 2.5 ng of cDNA template containing the appropriate primers (300 nmol/L) and SYBR Green PCR master mix (Applied BioSystems). Primers for each gene were obtained from distinct exons that spanned an intron by using the Ensembl Genome Browser program (<http://www.ensembl.org>). The sequence specificity of each primer was verified with the Blast program derived from the National Center for Biotechnology Information (<http://www.ncbi.nlm.nih.gov>). The primers used were as follows: for rat β -actin, forward 5'-AGGCTCTCTTCCAGCCTTCC-3' and reverse 5'-CATGG-ATGCCACAGGATTCC-3'; for rat nestin, forward 5'-TGCAGGCCACTGATAA-GTTCCA-3' and reverse 5'-TTCTCCTGCTCCAGGGCTTCCA-3'; for rat collagen type I, forward 5'-CTGACGCATGGCCAAGAAGACA-3' and reverse

5'-CGTGCCATTGTGGCAGATACAGAT-3'; for rat GATA-4, forward 5'-ATGGCACAGCAGCTCCA-3' and reverse 5'-CATGGCCGGACACAGTACTG-3'; for rat MEF-2C, forward 5'-GCCATCTGCCCTCAGTCAGT-3' and reverse 5'-TGAGATAAATGAGTGCTAGTGCAAGC-3'; for rat Nkx-2.5, forward 5'-CAAGGACCCTCGGGCG-3' and reverse 5'-TTTGTCCAGCTCCACCGC-3'; and for rat VEGF-A, forward 5'-GAAATCCCGGTTTAAATCCTGG-3' and reverse 5'-CGCTCTGAACAAGGCTCACAG-3'. Appropriate negative controls were used for each experiment.

Statistics

Data were presented as means \pm SE, where n represents the number of rats used in each experiment. Morphological and hemodynamic results were evaluated by a bilateral Student's unpaired T-test. Protein and mRNA expression were evaluated with a 1-way ANOVA and a significant difference was detected using the Neuman-Keuls post hoc test. A value of $P < 0.05$ is considered statistically significant.

RESULTS

1. The phenotype and presence of neural stem cells and nestin-immunoreactive cardiac myocyte-like cells in the infarcted rat and human heart.

In the normal rat heart, nestin immunoreactivity was detected exclusively in the neural stem cell population, marked by a refractive cell body and numerous processes, intercalated among terminally-differentiated connexin-43⁽⁺⁾ cardiac myocytes (Fig. 1). Neural stem cells did not stain positive for connexin-43, a gap junctional protein and marker of adult cardiac myocytes, whereas nestin was not expressed in adult cardiac myocytes. Following ischemic damage, neural stem cells were observed in the non-infarcted (Fig. 2A) and peri-infarct region (Fig. 2B) of the 3-week post-MI rats. Moreover, bordering the scar, structurally and morphologically immature nestin-immunoreactive cardiac myocyte-like cells were detected and expressed the cardiac specific marker desmin (Fig. 2B). Similarly, a rarity of nestin-immunoreactive cardiac myocyte-like cells has also been identified in the non-infarcted region (Fig. 2A). The underlying mechanisms attributed to their appearance remain presently undefined. The latter paradigm was not a transient response as nestin-immunoreactive cardiac myocyte-like cells (Fig. 3A, 3B & 3C) were detected in the peri-infarct/infarct region of 9-month post-MI rats. In contrast to the phenotype of cardiac myocytes residing in the viable myocardium (Fig. 4A), immunoreactivity of the gap junctional protein connexin-43 implicated in action potential propagation was either absent, lateralized or in the cytoplasm of nestin-immunoreactive cardiac myocyte-like cells (Fig. 4B). Phenotypically, these data demonstrate that structural and morphological immaturity nestin-

immunoreactive cardiac myocyte-like cells may represent a substrate for arrhythmogenesis (Rucker-Martin et al., 2006).

In the human infarcted heart, nestin-expressing cells were identified in the viable myocardium and scar and exhibited an identical anatomical phenotype to the population of neural stem cells residing in the infarcted rat heart (Fig. 6A & 6B). Concomitantly, structurally and morphologically immature nestin-immunoreactive cardiac myocyte-like cells were also detected in the infarcted human heart of 1-week post-MI patients (Fig. 6B) followed by a robust increase and maintenance of this cellular phenotype following 3 months post-MI (Fig. 6C & 6D). Furthermore, desmin immunoreactivity was detected in nestin-immunoreactive cardiac myocyte-like cells (Fig. 5A, 5B, 5C, & 5D). Lastly, akin to that reported in the rat infarcted heart, connexin-43 immunoreactivity was either absent, lateralized or in the cytoplasm of structurally and morphologically immature nestin-immunoreactive cardiac myocyte-like cells in the infarcted human heart (Fig. 6B, 6C, & 6D).

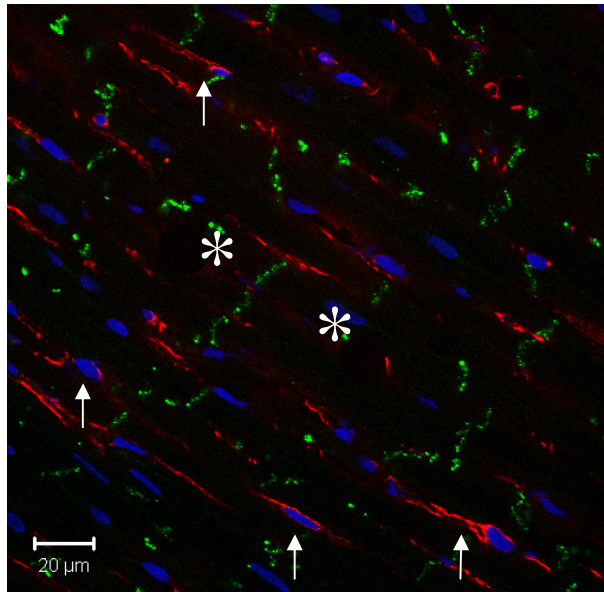


Fig. 1 - The absence of nestin-immunoreactive cardiac myocyte-like cells in the normal rat heart. Nestin immunoreactivity (red fluorescence) was detected in nestin⁽⁺⁾ neural stem cells (denoted by arrows) intercalated between nestin⁽⁻⁾ cardiac myocytes (denoted by *) that stained positive for the gap junctional protein connexin-43 (Cx43) (green fluorescence). The nucleus was identified with the blue fluorescent marker to-pro³.

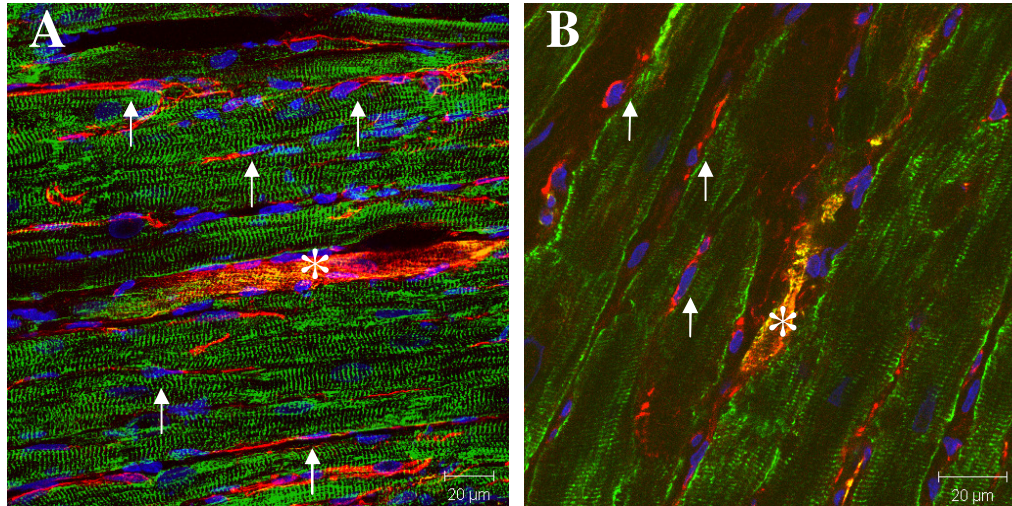


Fig. 2 - The presence of structurally and morphologically immature nestin⁽⁺⁾ cardiac myocyte-like cells in 3-week post-MI adult rats. A: Possible terminally differentiated nestin (red fluorescence) and desmin-immunoreactive (green fluorescence) cardiac myocyte-like cell (denoted by *) in the non-infarcted left ventricle with nestin⁽⁺⁾ neural stem cells (denoted by arrows). The underlying mechanisms attributed to its appearance remain undefined. B: Presence of structurally and morphologically immature nestin⁽⁺⁾/desmin⁽⁺⁾ cardiac myocyte-like cell in the peri-infarct region surrounded by nestin⁽⁺⁾ neural stem cells. The nucleus was identified with the blue fluorescent marker to-pro³.

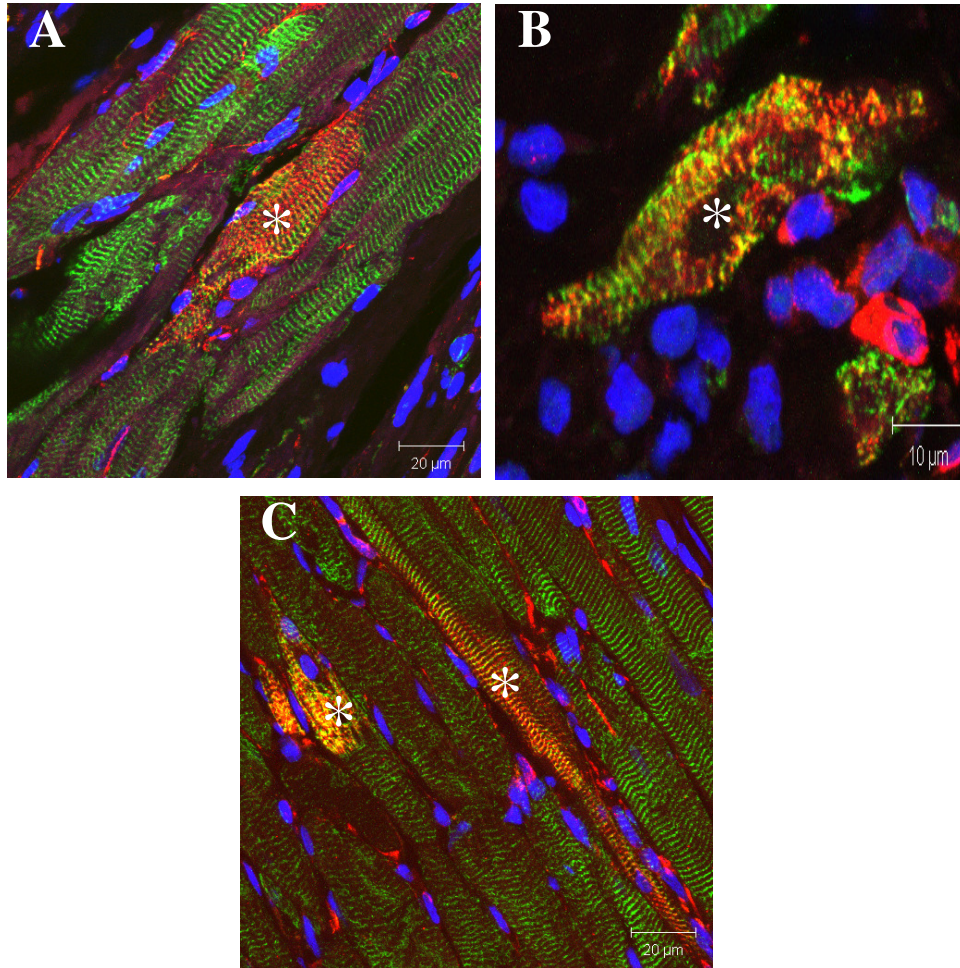


Fig. 3 - The presence of structurally and morphologically immature nestin⁽⁺⁾ cardiac myocyte-like cells in 9-month post-MI adult rats. A: Nestin⁽⁺⁾ (red fluorescence) and desmin⁽⁺⁾ (green fluorescence) cardiac myocyte-like cell (denoted by *) observed after 9 months in the peri-infarct region reflects a non-transient response. B: Presence of structurally and morphologically immature nestin⁽⁺⁾/desmin⁽⁺⁾ (green fluorescence) cardiac myocyte-like cell in the infarct region. C: Nestin⁽⁺⁾/desmin⁽⁺⁾ cardiac myocyte-like cells detected in the peri-infarct region. The nucleus was identified with the blue fluorescent marker to-pro³.

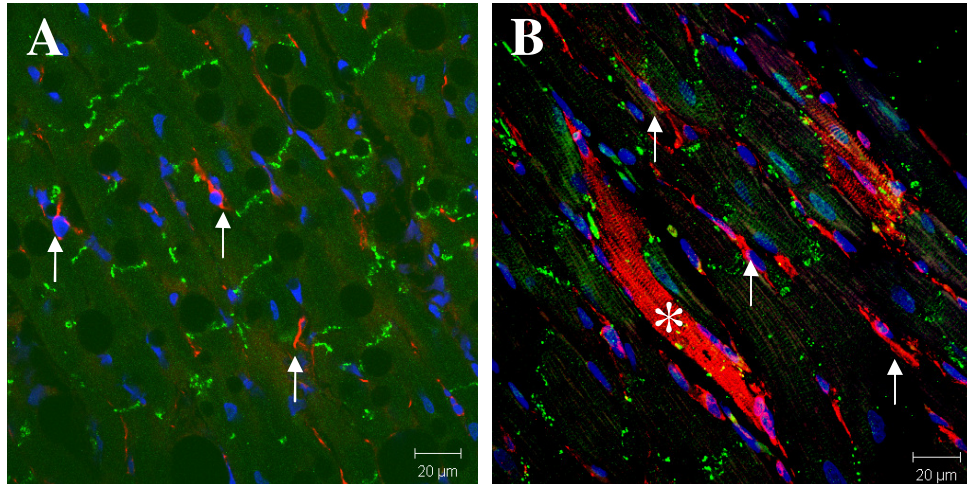


Fig. 4 - Connexin-43 organization in the heart of sham and 1-week post-MI rats. A: Cx43 (green fluorescence) is highly organized in the normal myocardium. Nestin⁽⁺⁾ (red fluorescence) neural stem cells (denoted by arrows) are present in the heart. B: An aberrant pattern of Cx43 staining, either lateralized or cytoplasmic, was detected in nestin⁽⁺⁾ cardiac myocyte-like cells (denoted by *). The nucleus was identified with the blue fluorescent marker to-pro³.

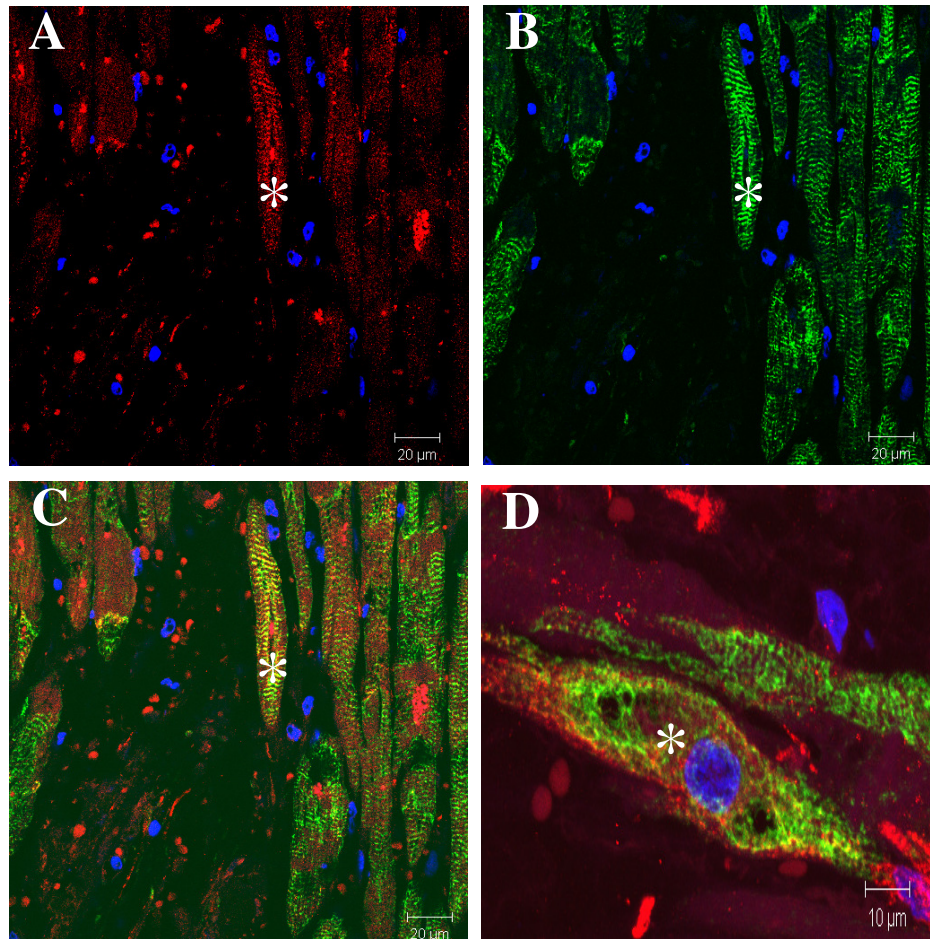


Fig. 5 - The presence of structurally and morphologically immature nestin⁽⁺⁾/desmin⁽⁺⁾ cardiac myocyte-like cells in the infarcted human heart. A: Nestin⁽⁺⁾ (red fluorescence) cardiac myocyte-like cell (denoted by *) in the infarct region. The same phenotypical myocyte-like cell was also observed in the infarcted rat heart. B: Desmin⁽⁺⁾ (green fluorescence) immunoreactivity of the same myocyte-like cell. C: Nestin and desmin co-localization. D: Structurally and morphologically immature nestin⁽⁺⁾/desmin⁽⁺⁾ cardiac myocyte-like cell forming in the scar. The nucleus was identified with the blue fluorescent marker to-pro³.

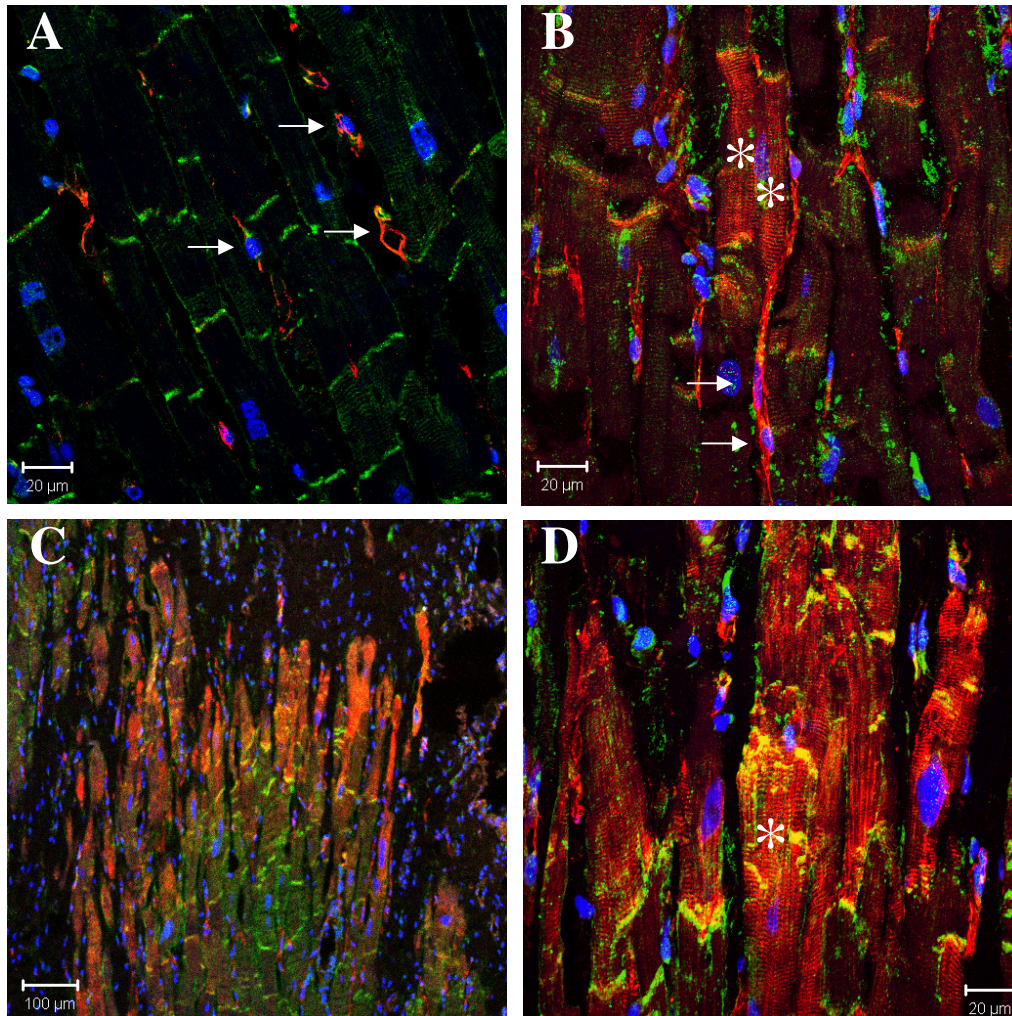


Fig. 6 - The presence of nestin⁽⁺⁾ cardiac myocyte-like cells in the infarcted human heart. A: Presence of nestin⁽⁺⁾ neural stem cells (red fluorescence) intercalated between cardiac myocytes in the viable myocardium of a 3 month post-MI patient. B: In 1 week post-MI, presence of nestin⁽⁺⁾ neural stem cells (denoted by arrows) and nestin⁽⁺⁾ cardiac myocyte-like cells (denoted by *) with aberrant connexin-43 (green fluorescence) staining. C: in 3 months post-MI, presence of nestin⁽⁺⁾/Cx43⁽⁺⁾ cardiac myocyte-like cells in the peri-infarct. D: In 3 month post-MI, nestin⁽⁺⁾/Cx43⁽⁺⁾ cardiac myocyte-like cell (denoted by *) in the peri-infarct with Cx43 lateralization. The nucleus was identified with the blue fluorescent marker to-pro³.

2. **Exposure of rat cardiac myocytes to hypoxia does not promote nestin expression.**

Unresolved issues include the source of nestin-immunoreactive cardiac myocyte-like cells and the stimulus implicated. The peri-infarct/infarct region represents a hypoxic environment (Wang et al., 2005) and it is tempting to speculate that hypoxia alone may induce the expression of nestin in surviving cardiac myocytes residing in this region. Therefore, the following experiments tested the hypothesis that nestin protein is induced in cardiac myocytes following exposure to hypoxia. The exposure of adult male Sprague-Dawley rats to normobaric hypoxia (12% O₂) for a period of 10 days failed to promote nestin expression in terminally differentiated cardiac myocytes (Fig. 7 & 8) and did not further lead to an increased expression in neural stem cells (Fig. 9B), as compared to rats exposed to ambient air (21% O₂) (Fig. 9A). Alternatively, it is possible that exposure of the rat to 12% O₂ did not adequately reflect the hypoxic milieu of the peri-infarct/infarct region. To circumvent this issue, isolated rat ventricular myocytes were exposed to 1% O₂ (normobaric hypoxia) for either 8 or 24 hours. Employing an immunofluorescence approach, nestin expression was not detected in connexin-43 immunoreactive rat ventricular myocytes (Fig. 10). By contrast, nestin immunoreactivity was detected in isolated cardiac neural stem cells. Furthermore, nestin mRNA expression was not increased in hypoxic rat ventricular myocytes (Fig. 11B), whereas VEGF mRNA levels were significantly elevated ($P < 0.05$) in neonatal ventricular myocytes following either an 8 (3.2 ± 0.5 -fold) or 24 hour (5.1 ± 0.9 -fold) exposure to hypoxia (Fig. 11A). Thus, collectively, these data suggest that hypoxia alone

cannot promote the reappearance of nestin-immunoreactive cardiac myocyte-like cells and cardiac myocytes do not represent the source of these cells in the myocardial infarcted rat heart.

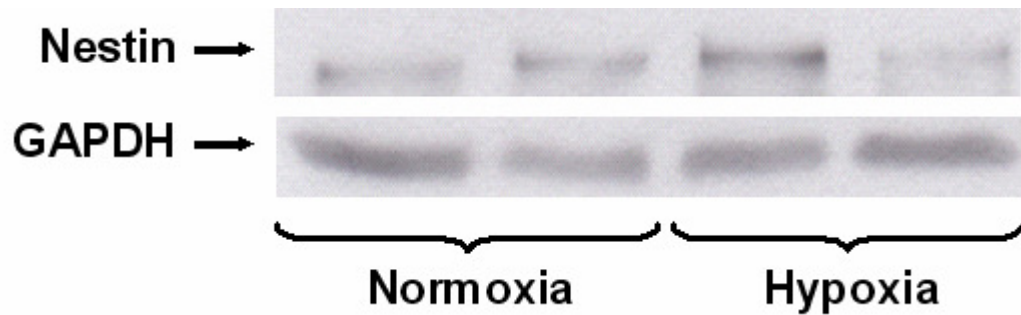


Fig. 7 - Nestin expression in the left and right ventricles of normoxic and hypoxic rats. In the hypoxic rats ($n = 2$), no significant change was detected in nestin expression in comparison to normoxic rats ($n = 2$). Nestin protein levels were normalized to GAPDH protein content.

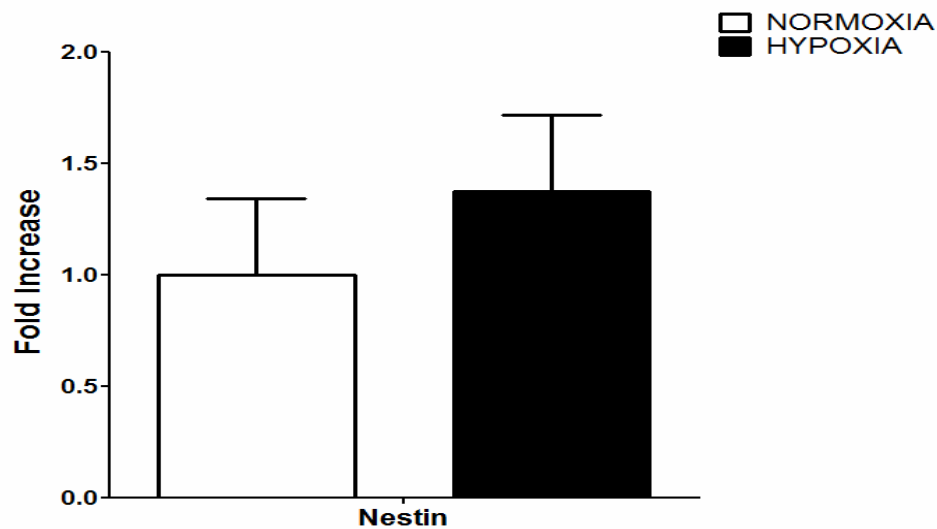


Fig. 8 - Quantitative analysis of nestin protein expression in normoxic and hypoxic rats. Nestin protein did not significantly increase in the left ventricle of the ISO-treated group ($n = 2$). Data are represented as fold increase vs. control group ($n = 2$). * $P < 0.05$ vs. control group. Data were evaluated by a 1-way ANOVA, and a significant difference was determined by Neuman-Keuls post hoc test.

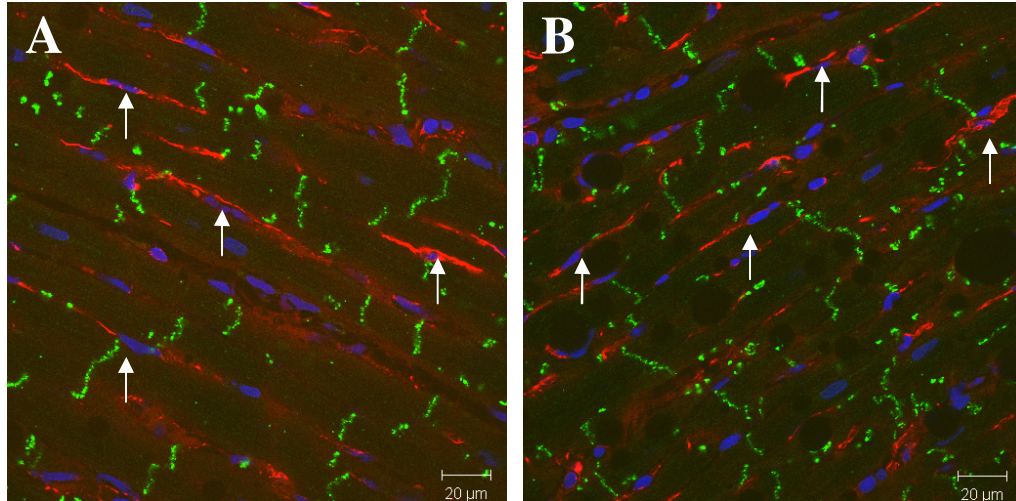


Fig. 9 - Nestin⁽⁺⁾ cardiac myocyte-like cells undetected in the myocardium following hypoxia. A: presence of nestin⁽⁺⁾ (red fluorescence) neural stem cells (denoted by arrows) in normoxic adult rats with connexin-43 (green fluorescence) identifying normal cardiac myocytes. B: continued presence of nestin⁽⁺⁾ neural stem cells in hypoxic adult rats with absence of nestin⁽⁺⁾ cardiac myocyte-like cells. The nucleus was identified with the blue fluorescent marker to-pro³.

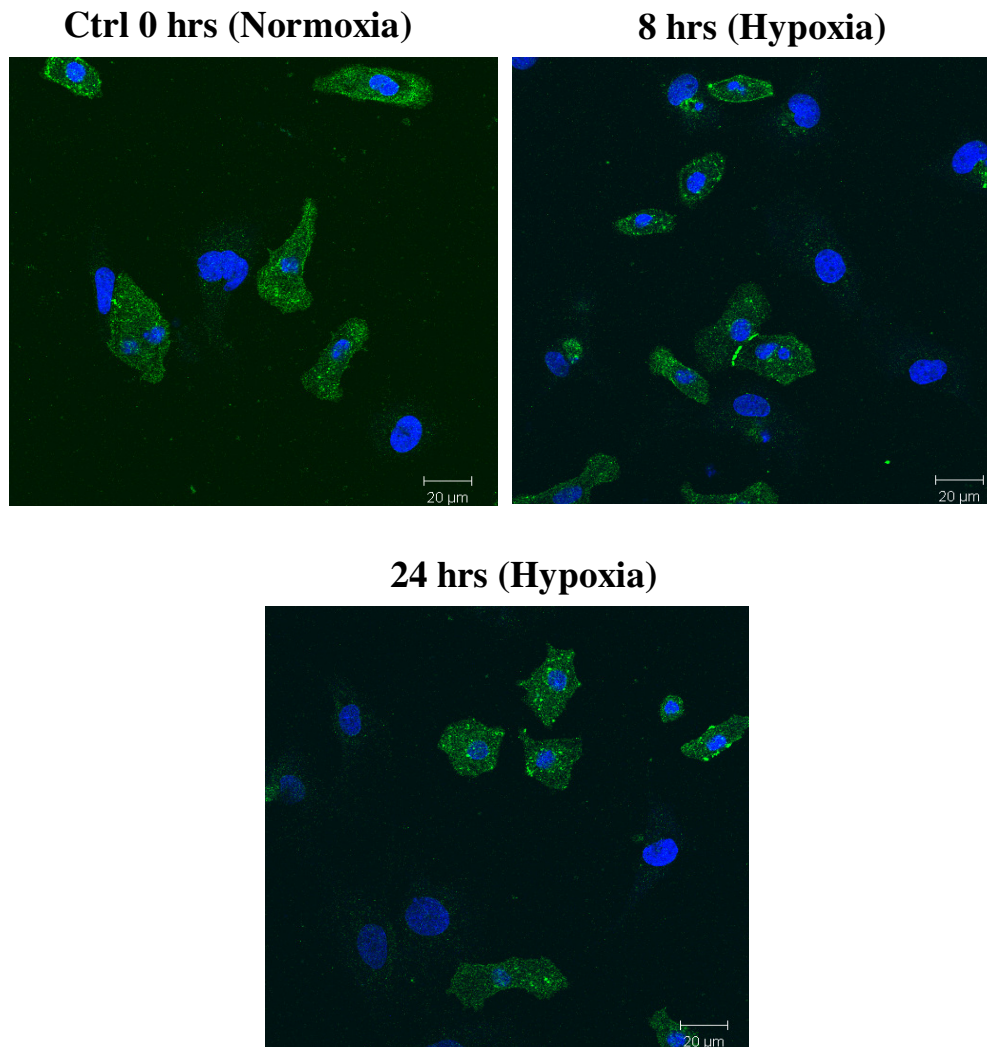


Fig. 10 - Nestin immunoreactivity (red fluorescence) not detected in Cx43⁽⁺⁾ (green fluorescence) neonatal ventricular cardiac myocytes following both normoxic and hypoxic exposures. The cells were exposed to 0, 8, and 24 hrs hypoxia treatment and nestin expression was not observed. The nucleus was identified with the blue fluorescent marker to-pro³.

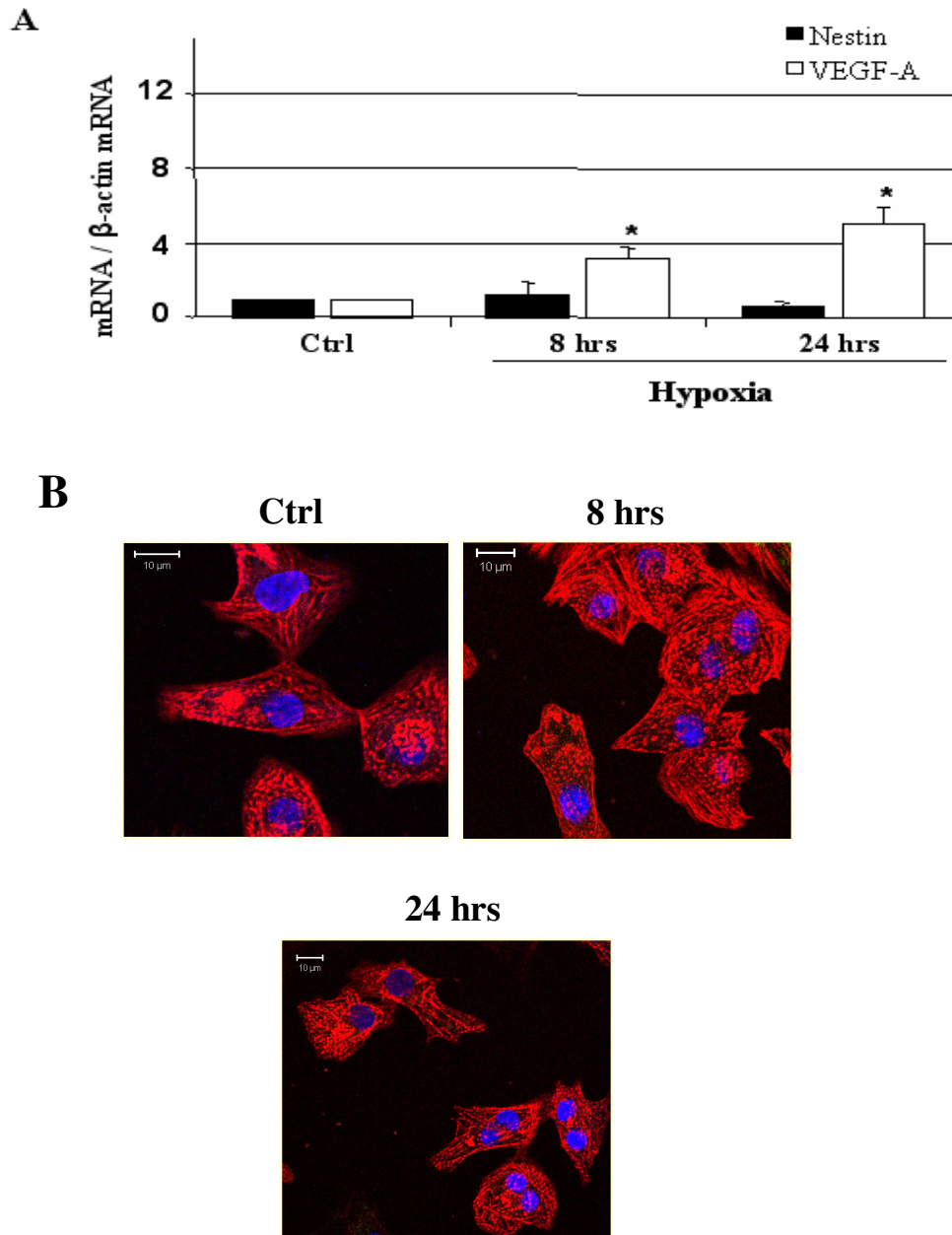


Fig. 11 - Effect of hypoxic exposure on neonatal cardiac myocytes. A: Nestin mRNA expression after hypoxia in neonatal cardiac myocytes. Employing real-time PCR, nestin mRNA was unchanged after hypoxia, whereas VEGF-A mRNA was significantly increased ($n = 4$) $P < 0.05$ (denoted by *) versus sham. Data were presented as the mean S.E.M, (n) represented independent preparations of neonatal cardiac myocytes, and mRNA levels normalized to β -actin mRNA. B: Nestin protein expression in neonatal cardiac myocytes. Nestin fluorescence was not detected after hypoxia whereas fluorescent phalloidin (red fluorescence), marking actin filaments, was observed.

3. Nestin-expressing cells in the normal rat heart express markers of cardiac progenitor cells.

The hypoxic experiments support the premise that hypoxia alone is insufficient to promote nestin expression in rat cardiac myocytes. Alternatively, hypoxia may be implicated but the absence of nestin protein induction in cardiac myocytes in response to a hypoxic stimulus *in vivo* or *in vitro* suggests that nestin-immunoreactive cardiac myocyte-like cells may originate from an alternative myocardial-derived population of cells. As a first step to address this issue, we examine whether a subpopulation of nestin-immunoreactive cells in the normal rat heart were associated with expression of markers associated with cardiac progenitor cells. First, mRNA expression of established markers of cardiac progenitor cells including, GATA-4, Nkx-2.5, and MEF-2C were detected in the normal adult rat heart (Fig. 12). GATA-4 staining was identified in the nucleus and cytoplasm of terminally differentiated cardiac myocytes, whereas Nkx-2.5 staining was not detected. Second, GATA-4 and Nkx-2.5 staining was detected in the cytoplasm of nestin-expressing cells in the normal rat heart (Fig. 13A & 13B). However, these transcriptional factors were not detected in the entire population, thereby demonstrating that at least two populations of nestin-expressing cells exist identified by the absence or presence of Nkx-2.5/GATA-4 (Fig. 13A & 13B). Furthermore, we also identified GATA-4/Nkx-2.5 immunoreactive cells that did not express nestin and detected intercalated among cardiac myocytes and the signal was detected predominantly in the cytoplasm (Fig. 13A & 13B). Thus, at least two populations of cells expressing markers of cardiac progenitor cells exist in the

normal rat heart distinguished by the absence or presence of nestin. These findings indirectly suggest that either population or both may be the source of nestin-immunoreactive cardiac myocyte-like cells following ischemic damage.

Cardiac Progenitor Marker Expression in Normal Adult Rat Hearts

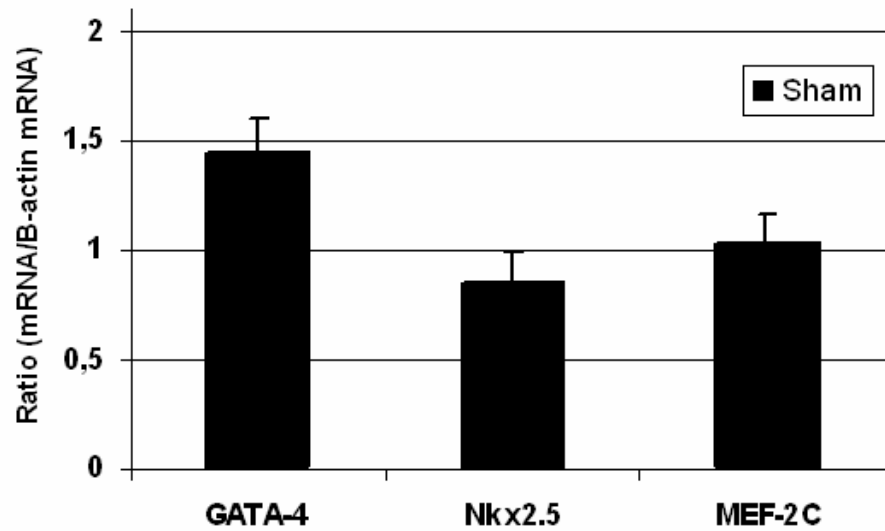


Fig. 12 - Cardiac progenitor cell marker expression in normal adult rat hearts. GATA-4, Nkx-2.5, and MEF-C expression were detected in sham group (n = 5) of rats.

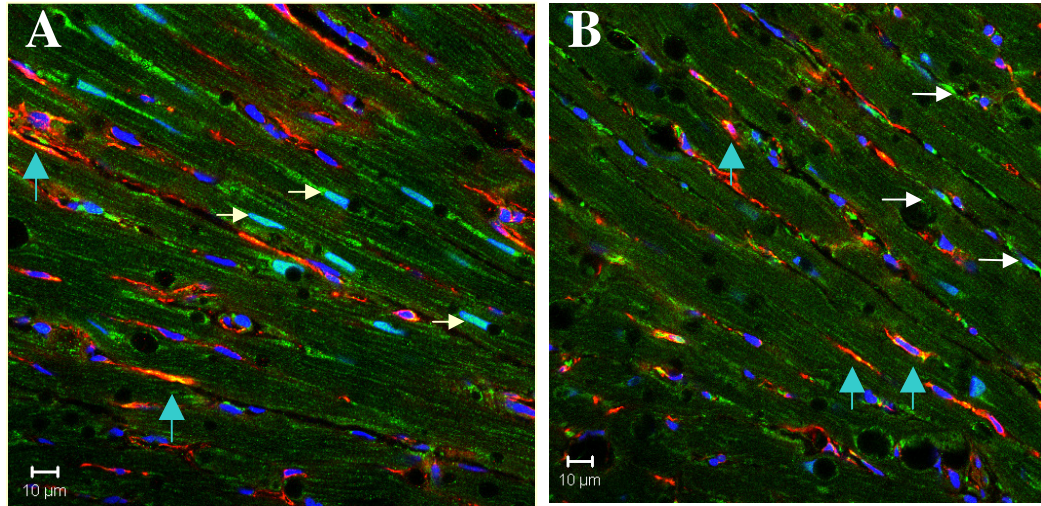


Fig. 13 - Distinguished subpopulations of nestin and cardiac progenitor stem cells are intercalated in between cardiac myocytes in the normal heart. A: nestin⁽⁺⁾ (red fluorescence) neural stem cells with a subpopulation of GATA-4⁽⁺⁾ (green fluorescence) cardiac progenitor cells (denoted by white arrows). In contrast, nestin⁽⁺⁾/GATA-4⁽⁺⁾ (denoted by blue arrows) cells have also been observed. B: Nestin⁽⁺⁾/Nkx-2.5⁽⁺⁾ (green fluorescence) (denoted by blue arrows) cells are detected in the normal heart with sparse Nkx-2.5⁽⁺⁾ cells (denoted by white arrows). The nucleus was identified with the blue fluorescent marker to-pro³.

4. β_1 -adrenergic receptor staining was detected in nestin-expressing cells.

Sympathetic hyperinnervation represents a common feature following myocardial infarction and our lab has demonstrated sympathetic fiber sprouting in the peri-infarct/infarct region of the ischemically damaged rat heart. These findings provided the impetus to assess whether the sympathetic system may contribute in part to the appearance of nestin-immunoreactive cardiac myocyte-like cells following myocardial infarction in the rat heart. Consistent with this premise, β_1 -adrenergic receptor immunoreactivity was ubiquitously detected in nestin-expressing cells residing in the normal rat heart (Fig. 14A & 14B). Thus, the population of nestin-expressing cells that express Nkx-2.5/GATA-4 represent a target of the sympathetic system. Therefore, these latter findings provided the impetus for the following experiment to examine whether isoproterenol infusion via osmotic pump implantation can promote the appearance of nestin-immunoreactive cardiac myocyte-like cells. Isoproterenol infusion significantly increased cardiac weight and the rate of left ventricular contraction and relaxation as compared to saline-infused rats (Table 1 & 2). Additional sham and ISO-treated rat hearts were utilized for hemodynamic measurements prior to usage for immunofluorescence and Sirius Red immunohistological staining. Furthermore, nestin protein expression was significantly increased in the heart of isoproterenol-treated rats compared to saline-treated rats (Fig. 16 & 17). Employing an immunofluorescence approach, structurally and morphologically immature nestin- and β_1 AR-immunoreactive cardiac myocyte-like cells were identified in the heart of

isoproterenol-treated rats (Fig. 14C, 14D, 15A, 15B, 15C, & 15D). However, the preponderance of structurally and morphologically immature nestin-immunoreactive cardiac myocyte-like cells was detected in close proximity to or within localized regions of apparent tissue death. Consistent with these findings, the apoptotic protein Bax and anti-apoptotic protein Bcl-2 significantly increased in the heart of isoproterenol-treated rats (Fig. 16 & 17). Furthermore, extensive fibrosis was detected throughout the left ventricle following isoproterenol administration using Sirius Red immunohistological staining (Fig. 18B) as a 6-fold increase in collagen content was detected as compared to sham rats (Fig. 18A). Consistent with these data, left ventricular collagen α_1 type 1 mRNA expression was significantly increased as compared to sham rats (Fig. 19).

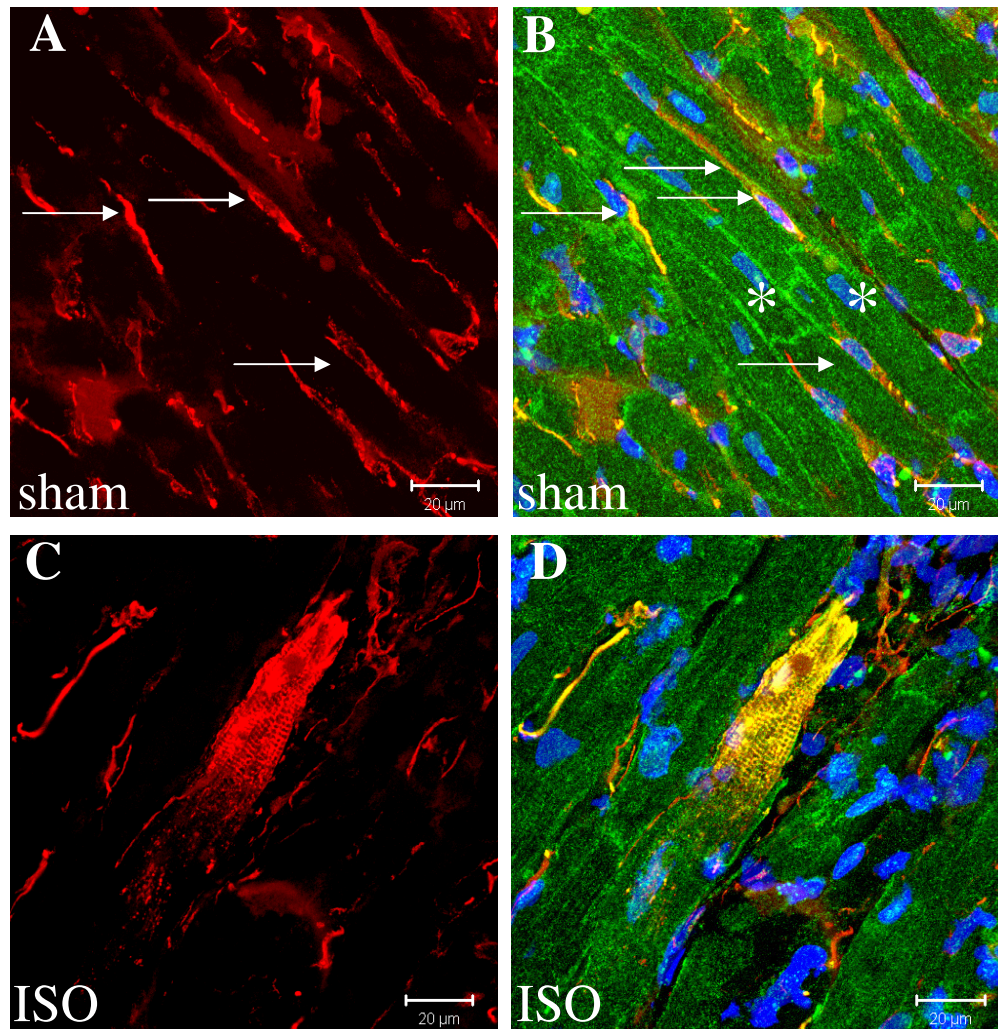


Fig. 14 - β_1 -adrenergic receptor (β_1 AR) immunoreactivity in nestin⁽⁺⁾ stem cells and nestin⁽⁺⁾ cardiac myocyte-like cells. A: nestin (red fluorescence) depicting the nestin⁽⁺⁾ stem cell population. B: cytoplasmic β_1 AR (green fluorescence) immunoreactivity in the nestin⁽⁺⁾ stem cells (denoted by arrows) and β_1 AR immunoreactivity was also observed on the plasma membrane of cardiac myocytes (denoted by *). C: appearance of nestin⁽⁺⁾ cardiac myocyte-like cell. D: membrane and nuclear expression of β_1 ARs in nestin⁽⁺⁾ cardiac myocyte-like cells. The nucleus was identified with the blue fluorescent marker to-pro³.

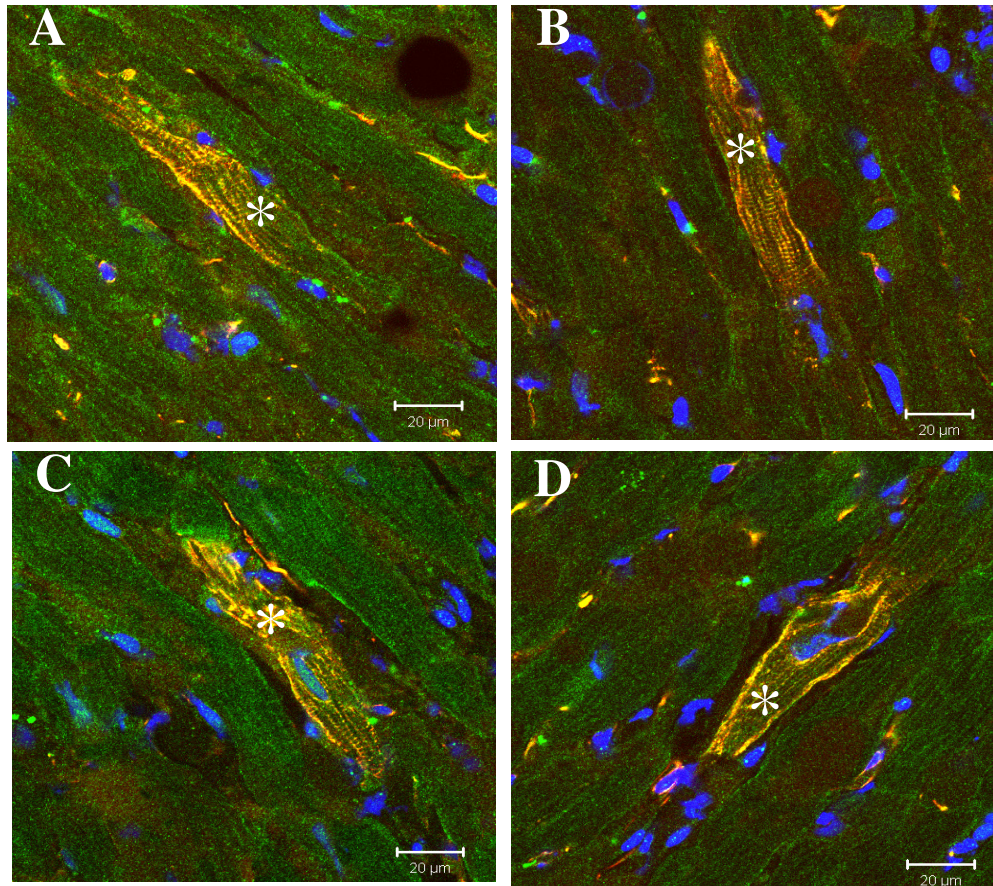


Fig. 15 - Numerous nestin⁽⁺⁾ cardiac myocyte-like cells expressing β_1 -adrenergic receptors (β_1 ARs) in ISO-treated rats. A, B, C, D: the nestin⁽⁺⁾ cardiac myocyte-like cells (denoted by *) following ISO-delivery are maintaining β_1 AR expression while the neighboring normal cardiac myocytes have downregulated their β_1 AR expression.

Table 1. *Body and heart weights of sham and 1-week ISO-treated rats*

	BW, g	Heart, g	LV, mg	LV/BW, mg/g	RV, mg	RV/BW, mg/g
Sham (n = 6)	364 ± 7	1130 ± 38	538 ± 20	1.48 ± 0.05	175 ± 8	0.48 ± 0.02
ISO (n = 5)	350 ± 11	1455 ± 100**	665 ± 40*	1.89 ± 0.06***	234 ± 18*	0.67 ± 0.05**

Data are presented as means ± SE; n = no. of rats examined. ISO, isoproterenol; BW, body weight; LV, left ventricle; RV, right ventricle. *P < 0.05 vs. sham. **P < 0.01 vs. sham. ***P < 0.001 vs. sham. Data were evaluated and a significant difference was determined by Student's unpaired T-test.

Table 2. *Hemodynamic parameters of sham and 1-week ISO-treated rats*

	LVSP, mmHg	LVEDP, mmHg	LV +dP/dt, mmHg/s	LV -dP/dt, mmHg/s
Sham (n = 12)	153 ± 9	11 ± 1	7048 ± 253	6036 ± 311
ISO (n = 10)	153 ± 9	17 ± 2*	9072 ± 453***	7275 ± 518*

Data are presented as means ± SE; n = no. of rats examined. ISO, isoproterenol; LVSP, left ventricular systolic pressure; LVEDP, left ventricular end-diastolic pressure; LV +dP/dt, rate of LV contraction; LV -dP/dt, rate of LV relaxation. *P < 0.05 vs. sham. ***P < 0.001 vs. sham. Data were evaluated and a significant difference was determined by Student's unpaired T-test.

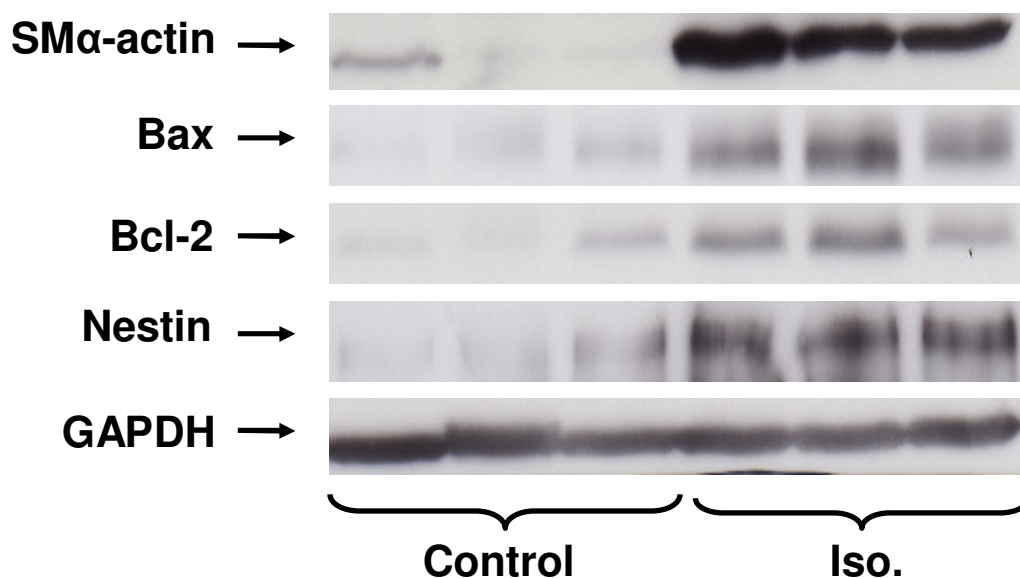


Fig. 16 - Smooth muscle α -actin, Bax, Bcl-2, and nestin expression in the left ventricle of sham and ISO-treated rats. In the ISO-treated rats, smooth muscle α -actin, Bax, Bcl-2, and nestin increased significantly in the left ventricle following isoproterenol administration compared to sham rats. SMA-actin, Bax, Bcl-2 and nestin protein levels were normalized to GAPDH protein content.

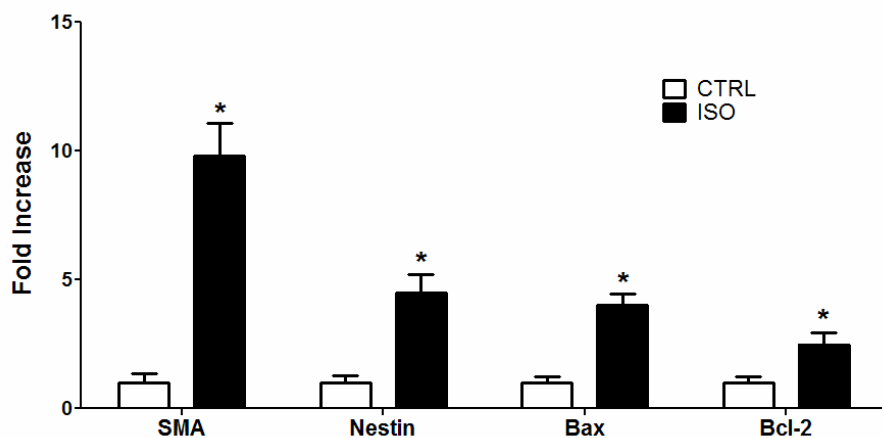


Fig. 17 - Quantitative analysis of protein expression in the left ventricle of sham and isoproterenol-treated rats. Smooth muscle α -actin, nestin, Bax, and Bcl-2 protein were significantly increased in the left ventricle of the ISO-treated group ($n = 5$). The increase in Bax confirms the onset of apoptosis in the ISO-treated group, followed by concurrent fibrotic response substantiated by the rise in SMA. Data are represented as fold increase vs. sham group ($n = 6$). * $P < 0.05$ vs. sham group. Data were evaluated by a 1-way ANOVA, and a significant difference was determined by Neuman-Keuls post hoc test.

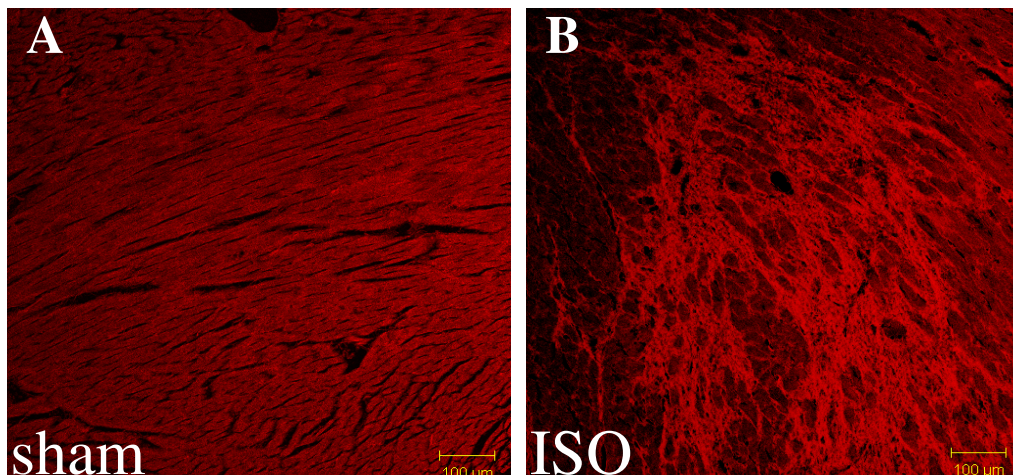


Fig. 18 - Sirius Red immunohistological staining of collagen in the left ventricle of sham and ISO-treated rats. A: No visible signs of fibrosis detected in the myocardium of sham rats. B: Extensive fibrosis in the heart of ISO-treated rats as reflected by increased collagen deposition.

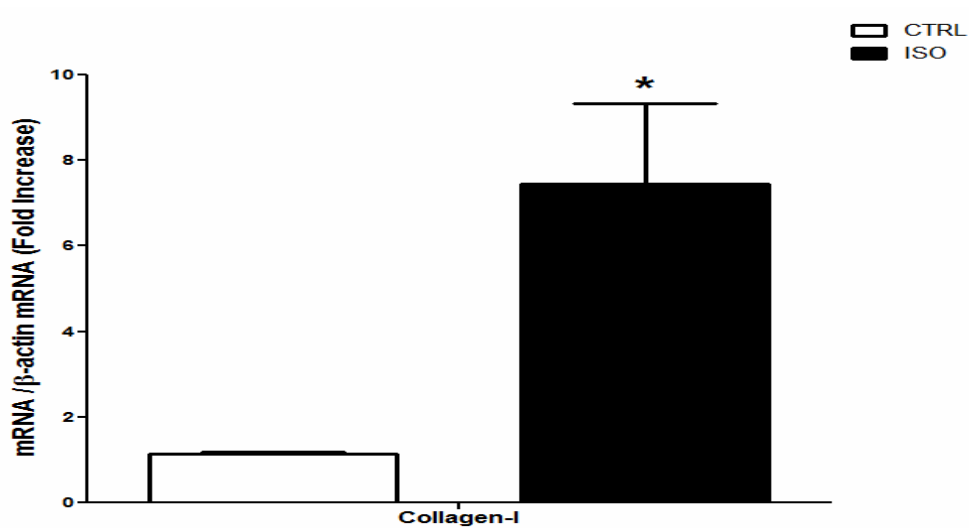


Fig. 19 - Collagen mRNA expression in the left ventricle of sham and isoproterenol-treated rats. Collagen α 1 type 1 mRNA increased significantly, thus indicative of the onset of fibrosis in the left ventricle of ISO-treated rats ($n = 4$) compared to sham rats ($n = 6$). Data are represented as fold increase vs. sham rats. * $P < 0.05$ vs. sham rats. Data were evaluated by a 1-way ANOVA, and significant difference was determined by the Neuman-Keuls post hoc test.

DISCUSSION

Scar formation following ischemic damage to the heart represents an essential physiological response and is denoted as reparative fibrosis (El-Helou et al., 2005). The biological events associated with reparative fibrosis include inflammation, the differentiation of a fibroblast to a myofibroblast and subsequent deposition of collagen, and angiogenesis (Frangogiannis NG, 2008). Work from Calderone's group and others have recently demonstrated that sympathetic fiber sprouting and innervation of the peri-infarct/infarct region represents a conserved event of healing in the ischemically damaged heart (Vracko et al., 1990; Zhang et al., 2001; Drapeau et al., 2005; Zhou et al., 2004; El-Helou et al., 2005). The postulated biological role of the sympathetic system during reparative fibrosis may involve coordinating angiogenesis and myofibroblast proliferation. Lastly, Calderone's group made the novel observation that the rat heart contained a resident population of neural stem cells that migrated to the infarct region following ischemic injury (Drapeau et al., 2005). In the infarct region, a subpopulation of these neural stem cells may represent a novel cellular substrate for *de novo* blood vessel formation, thereby contributing to the intrinsic angiogenic response in the scar (El-Helou et al., 2008). During the latter studies, an unexpected observation was the appearance of nestin-immunoreactive cardiac myocyte-like cells bordering the infarct region. These nestin-immunoreactive cardiac myocyte-like cells were structurally and morphologically immature as compared to terminally differentiated cardiac myocytes and appeared to be in a state of differentiation. These findings indirectly supported the basis of a plausible intrinsic self-regeneration capacity of the heart where new cardiac myocytes are identified by nestin expression. In the

normal rat heart and viable myocardium of an MI rat heart, cardiac myocytes do not express nestin. These observations were recently reaffirmed by Scobioala et al. (2008), as nestin-immunoreactive cardiac myocyte-like cells were detected in the peri-infarct region of the infarcted mouse heart. Lastly, these nestin-immunoreactive cardiac myocyte-like cells were also identified in the infarcted human heart (Mokry et al., 2008; El-Helou et al., 2008). Thus, these data have provided the impetus to examine the phenotype and origin of these nestin-immunoreactive cardiac myocyte-like cells and identify the stimuli implicated in their appearance.

The appearance of structurally and morphologically immature nestin-immunoreactive cardiac myocyte-like cells during the early phase of scar formation in the rat heart was not a transient response, as these cells were identified 9 months post-MI. Concomitantly, these nestin-immunoreactive cardiac myocyte cells were also detected in the peri-infarct/infarct regions of the ischemically damaged human heart and were detected at least 3 months after myocardial infarction. These data suggest that the persistent presence of nestin-immunoreactive cardiac myocyte-like cells may represent an important aspect in scar healing. However, the biological role of these cells in reparative fibrosis remains presently undefined. Furthermore, the co-expression of the intermediate filament desmin, connexin-43, and the emergence of a striated phenotype reaffirmed the premise that these nestin-immunoreactive cardiac myocyte-like cells reflected a cardiac myocyte phenotype. However, the staining pattern of connexin-43, a cardiac myocyte gap junctional

protein implicated in action potential propagation, was aberrant. In either the normal rat heart or the viable myocardium of an infarcted rat heart, connexin-43 immunoreactivity was detected intercalated at gap junctions between cardiac myocytes. By contrast, in structurally and morphologically immature nestin-immunoreactive cardiac myocyte-like cells, connexin-43 staining was absent, in the cytoplasm or lateralized. A similar paradigm was also observed in nestin-immunoreactive cardiac myocyte-like cells identified in the infarcted human heart. The aberrant pattern of connexin-43 expression in this subpopulation of cells bordering the peri-infarct may represent an underlying mechanism attributed to the reported arrhythmogenesis following myocardial infarction (Amino et al., 2006). Furthermore, a recent study by Rucker-Martin et al. (2006), reported that connexin-43 lateralization on cardiac myocytes may represent an important contributor to the genesis of arrhythmias. Thus, the aberrant pattern of connexin-43 in a subpopulation of cardiac myocyte-like cells that selectively express nestin may represent a novel substrate contributing to arrhythmogenesis and sudden cardiac death following ischemic damage.

It has been well established that the peri-infarct/infarct region is a hypoxic environment secondary to an inadequate angiogenic response (Lee et al., 2000). During the early phase of scar formation, structurally and morphologically immature nestin-immunoreactive cardiac myocyte-like cells were identified predominantly in the peri-infarct/infarct region. These observations provided the impetus to suggest that the hypoxic environment of the peri-infarct/infarct region

may have initiated the induction of nestin in surviving cardiac myocytes. To directly test this premise, normal male adult Sprague-Dawley rats were exposed to normobaric hypoxia (12% O₂) for 10 days whereas the sham group was exposed to ambient air (21% O₂). The exposure of rats to hypoxia failed to promote the reappearance of nestin-immunoreactive cardiac myocyte-like cells. Furthermore, nestin protein content in the heart of hypoxic rats was similar to sham further suggesting that hypoxia did not influence the resident cardiac neural stem cell population. Thus, these data suggest that a hypoxic environment was insufficient to initiate the appearance of nestin-immunoreactive cardiac myocyte-like cells. Alternatively, it is possible that a hypoxic environment of 12% O₂ was not comparable to that of the infarct region and therefore, inadequate to promote nestin expression in cardiac myocytes. To resolve the latter issue, neonatal rat ventricular myocytes were exposed to 1% O₂ and despite a near anoxic environment, neither nestin protein nor mRNA were expressed. However, as a positive control, VEGF mRNA levels were significantly increased, as the promoter region of the gene contains the hypoxia response element (HRE) (Breen et al., 2008). Collectively, these data support the premise that the exposure to hypoxia alone was insufficient to promote the reappearance of nestin-immunoreactive cardiac myocyte-like cells in the adult rat heart or isolated neonatal rat ventricular myocytes. Furthermore, cardiac myocytes did not appear to represent the cellular source of nestin-immunoreactive cardiac myocyte-like cells. In this regard, an alternative myocardial-derived population of cells recruited following an ischemic insult may differentiate to a nestin-immunoreactive cardiac myocyte-like cell.

The work from Anversa's group identified a population of cardiac progenitor cells that expressed the transcriptional factors Nkx-2.5 and GATA-4 (Beltrami et al., 2003). These transcriptional factors were reported to contribute to cardiac myocyte differentiation during development (Jamali et al., 2001). However, these studies failed to examine whether these Nkx-2.5/GATA-4 cardiac progenitor cells express nestin. Furthermore, it remains unknown if the population of nestin-immunoreactive cardiac myocyte-like cells that were identified in the infarcted rat or human heart initially expressed nestin and subsequently differentiated to a cardiac myocyte-like cell or if nestin was induced during differentiation. Thus, as a first approach, we examined if a subpopulation of nestin-expressing cells in the normal rat heart expressed the cardiac progenitor markers Nkx-2.5/GATA-4. Indeed, Nkx-2.5 and GATA-4 immunoreactivity was identified in a subpopulation of nestin-expressing cells that resembled anatomically the neural stem cell population. However, nestin-immunoreactive neural stem cells were also identified that lacked Nkx-2.5/GATA-4 staining. Therefore, these data suggest that the heart contains at least two populations of nestin-expressing cells distinguished by the absence or presence of Nkx-2.5/GATA-4. It remains presently unknown if either population may represent the source of nestin-immunoreactive cardiac myocyte-like cells. Interestingly, the study by Tomita et al. (2005), likewise identified a nestin population of cells in the mouse heart that exhibited characteristics of a neural stem cell. Furthermore, the injection of these mouse-derived nestin-expressing cells in the heart differentiated to a cardiac myocyte. In this regard, these latter data indirectly suggest that nestin-expressing cells that contain Nkx-2.5/GATA-4 may

indeed be recruited following ischemic damage and differentiate to a cardiac myocyte-like cell. Lastly, we also identified Nkx-2.5/GATA-4 cells intercalated among cardiac myocytes in the normal rat heart that lacked nestin expression. In our studies, we did not examine if the latter population expressed c-kit, an additional marker of cardiac progenitor cells reported by Anversa's group (Beltrami et al., 2003). However, it is also possible that these nestin-negative Nkx-2.5/GATA-4 cells may be recruited following an ischemic insult and during differentiation to a cardiac myocyte-like cell expresses nestin.

Work from Calderone's group and others have demonstrated that newly formed sympathetic fibers innervate the peri-infarct/infarct region and may play a seminal role in scar healing (Vracko et al., 1990; Zhang et al., 2001; Drapeau et al., 2005; Zhou et al., 2004; El-Helou et al., 2005). Thus, based on the latter findings and the presence of nestin-immunoreactive cardiac myocyte-like cells in the peri-infarct/infarct region, we tested the hypothesis that sympathetic system may be involved in their reappearance following an ischemic insult. In support of this premise, β_1 -adrenergic receptor staining was detected ubiquitously in the nestin-immunoreactive neural stem cell population. Therefore, nestin-immunoreactive neural stem cells that express Nkx-2.5/GATA-4 may represent a target of the sympathetic system. The infusion of the non-selective β -adrenergic agonist isoproterenol in the normal male adult rat heart significantly increased cardiac weight, heart rate, and contractility. Furthermore, nestin protein expression was significantly increased in isoproterenol-treated rats compared to vehicle-treated rats.

Employing an immunofluorescence approach, the global presence of nestin-immunoreactive cardiac myocyte-like cells was not observed in the heart of isoproterenol-treated rats. By contrast, a paucity of nestin-immunoreactive cells was detected in regions associated with tissue loss. The latter finding is not unexpected as several studies have reported the apoptotic action of β -adrenergic agonists on cardiac myocytes (Krishnamurthy et al., 2007; Menon et al., 2006). Indeed, consistent with these findings, the apoptotic protein Bax and the anti-apoptotic protein Bcl-2 were significantly increased in the heart of isoproterenol-treated rats. Furthermore, extensive fibrosis was detected throughout the myocardium following isoproterenol administration and confirmed by the significant increase of left ventricular collagen content. Collectively, these data suggest that the appearance of nestin- and β_1 AR-immunoreactive cardiac myocyte-like cells represents a compensatory response to the loss of cardiac myocytes initiated by isoproterenol-mediated cardiac myocyte apoptosis. In addition, in our opinion, the significant increase of nestin protein expression in isoproterenol-treated rats was not secondary to the paucity of nestin-immunoreactive cardiac myocyte-like cells detected in these hearts. By contrast, the increase expression of nestin may be directly related to β -adrenergic-mediated neural stem cell proliferation. Lastly, β_1 -adrenergic receptor immunoreactivity was markedly reduced in adult cardiac myocytes following isoproterenol treatment and was consistent with the premise of G-protein coupled receptor downregulation following chronic agonist exposure (Karoor et al., 1996). By contrast, β_1 -adrenergic receptor expression remained persistent in nestin-immunoreactive cardiac myocyte-like cells and neural

stem cells. The underlying mechanism(s) associated with the refractive nature of these cells to maintain β_1 -adrenergic receptor following isoproterenol treatment remains presently unknown. However, the expression of the β_1 -adrenergic receptor coupled to aberrant connexin-43 immunoreactivity in these phenotypically immature nestin-immunoreactive cardiac myocyte-like cells further corroborates the arrhythmogenic premise of the cells as in the infarcted heart model.

CONCLUSION

Our study is the first to demonstrate the appearance of nestin⁽⁺⁾ cardiac myocyte-like cells bordering the infarct region of both rat and human infarcted hearts. Their reappearance is not a transient response since nestin⁽⁺⁾ cardiac myocyte-like cells were detected in 3- and 9-month post-MI human and rat hearts, respectively. Aberrant connexin-43 staining coupled to the presence of the β_1 -adrenergic receptor in these nestin⁽⁺⁾ cardiac myocyte-like cells suggests that this subpopulation of cells may represent a novel substrate for arrhythmogenesis following an ischemic insult. The exposure of either the rat or isolated ventricular myocytes to hypoxia failed to stimulate nestin expression in terminally differentiated cardiac myocytes. Therefore, these data suggest that nestin⁽⁺⁾ cardiac myocyte-like cells may originate from a resident cardiac progenitor stem cell pool. Indeed, we detected a subpopulation of nestin-expressing cells in the normal rat heart that expressed the cardiac progenitor markers Nkx-2.5 and GATA-4. Therefore, it is possible that the reappearance of nestin⁽⁺⁾ cardiac myocyte-like cells following ischemic injury may be derived at least in part from nestin/Nkx-2.5/GATA-4 immunoreactive cells. An important issue that was not addressed in the present thesis is the biological role of these nestin⁽⁺⁾ cardiac myocyte-like cells. Our prevailing hypothesis is that the reappearance of these nestin⁽⁺⁾ cardiac myocyte-like cells represents an adaptive physiological response that attempts to replace the lost population of cardiac myocytes following myocardial infarction. Therefore, identifying stimuli implicated in the reappearance of nestin⁽⁺⁾ cardiac myocyte-like cells may represent a potential therapeutic approach to limit infarct expansion following an ischemic insult.

REFERENCES

1. Amoh Y, Li L, Yang M, Moossa AR, Katsuoka K, Penman S, Hoffman RM. Nascent blood vessels in the skin arise from nestin-expressing hair follicle cells. *Proc Natl Acad Sci U S A*. 2004 Sep 7;101(36):13291-5.
2. Amino M, Yoshioka K, Tanabe T, Tanaka E, Mori H, Furusawa Y, Zareba W, Yamazaki M, Nakagawa H, Honjo H, Yasui K, Kamiya K, Kodama I. Heavy ion radiation up-regulates Cx43 and ameliorates arrhythmogenic substrates in hearts after myocardial infarction. *Cardiovasc Res*. 2006 Dec 1;72(3):412-21.
3. Asano A, Morimatsu M, Nikami H, Yoshida T, Saito M. Adrenergic activation of vascular endothelial growth factor mRNA expression in rat brown adipose tissue: implication in cold-induced angiogenesis. *Biochem J*. 1997 Nov 15;328(Pt 1):179-83.
4. Beltrami AP, Barlucchi L, Torella D, Baker M, Limana F, Chimenti S, Kasahara H, Rota M, Musso E, Urbanek K, Leri A, Kajstura J, Nadal-Ginard B, Anversa P. Adult cardiac stem cells are multipotent and support myocardial regeneration. *Cell*. 2003 Sep 19;114(6):763-76.
5. Borisov AB, Huang SK, Carlson BM. Remodeling of the vascular bed and progressive loss of capillaries in denervated skeletal muscle. *Anat Rec*. 2000 Mar 1;258(3):292-304.

6. Booz GW, Baker KM. Molecular signalling mechanisms controlling growth and function of cardiac fibroblasts. *Cardiovasc Res.* 1995 Oct;30(4):537-43.
7. Breen E, Tang K, Olfert M, Knapp A, Wagner P. Skeletal muscle capillarity during hypoxia: VEGF and its activation. *High Alt Med Biol.* 2008 Summer;9(2):158-66.
8. Brodde OE. Beta 1- and 2-adrenoceptors in the human heart: properties, function, and alterations in chronic heart failure. *Pharmacol Rev.* 1991 Jun;43(2):203-42.
9. Chang F, Lee JT, Navolanic PM, Steelman LS, Shelton JG, Blalock WL, Franklin RA, McCubrey JA. Involvement of PI3K-Akt pathway in cell cycle progression, apoptosis, and neoplastic transformation: a target for cancer chemotherapy. *Leukemia.* 2003 Mar;17(3):590-603.
10. Chesley A, Lundberg MS, Asai T, Xiao RP, Ohtani S, Lakatta EG, Crow MT. The beta(2)-adrenergic receptor delivers an antiapoptotic signal to cardiac myocytes through G(i)-dependent coupling to phosphatidylinositol 3'-kinase. *Circ Res.* 2000 Dec 8;87(12):1172-9.

11. Communal C, Singh K, Pimentel DR, Colucci WS. Norepinephrine stimulates apoptosis in adult rat ventricular myocytes by activation of the beta-adrenergic pathway. *Circulation*. 1998 Sep 29;98(13):1329-34.
12. Communal C, Singh K, Sawyer DB, Colucci WS. Opposing effects of beta(1)- and beta(2) adrenergic receptors on cardiac myocyte apoptosis: role of pertussis toxin-sensitive G protein. *Circulation*. 1999 Nov 30;100(22):2210-2.
13. Donovan MJ, Lin MI, Wiegand P, Ringstedt P, Kraemer R, Hahn R, Wang S, Ibanez CF, Rafii S, Hempstead BL. Brain derived neurotrophic factor is an endothelial cell survival factor required for intramyocardial vessel stabilization. *Development*. 2000 Nov;127(21):4531-40.
14. Drapeau J, El-Helou V, Clement R, Bel-Hadj S, Gosselin H, Trudeau LE, Villeneuve L, Calderone A. Nestin-expressing neural stem cells identified in the scar following myocardial infarction. *J Cell Physiol*. 2005 Jul;204(1):51-62.
15. El-Helou V, Dupuis J, Proulx C, Drapeau J, Clement R, Gosselin H, Villeneuve L, Manganas L, Calderone A. Resident nestin+ neural-like cells and fibers are detected in normal and damaged rat myocardium. *Hypertension*. 2005 Nov;46(5):1219-25.

16. El-Helou V, Proulx C, Gosselin H, Clement R, Mimee A, Villeneuve L, Calderone A. Dexamethasone treatment of post-MI rats attenuates sympathetic innervation of the infarct region. *J Appl Physiol.* 2008 Jan;104(1):150-6.
17. El-Helou V, Beguin PC, Assimakopoulos J, Clement R, Gosselin H, Brugada R, Aumont A, Biernaskie J, Villeneuve L, Leung TK, Fernandes KJ, Calderone A. The rat heart contains a neural stem cell population; Role in sympathetic sprouting and angiogenesis. *J Mol Cell Cardiol.* 2008 Nov;45(5):694-702.
18. Emanuelli C, Salis MB, Pinna A, Graiani G, Manni L, Madeddu P. Nerve growth factor promotes angiogenesis and arteriogenesis in ischemic hindlimbs. *Circulation.* 2002 Oct 22;106(17):2257-62.
19. Frangogiannis NG. The immune system and cardiac repair. *Pharmacol Res.* 2008 Jun 24.
20. Gao MH, Lai NC, Roth DM, Zhou J, Zhu J, Anzai T, Dalton N, Hammond HK. Adenylyl cyclase increases responsiveness to catecholamine stimulation in transgenic mice. *Circulation.* 1999 Mar 30;99(12):1618-22.

21. Hausdorff WP, Caron MG, Lefkowitz, RJ. Turning off the signal: desensitization of beta-adrenergic receptor function. *FASEB J.* 1990 Aug;4(11):2881-9.
22. Heart and Stroke Foundation of Canada. Report Card 2004 - Fat is the New Tobacco.
23. Heart and Stroke Foundation of Canada. Tipping the Scales of Progress: 25. Heart Disease and Stroke in Canada. 2006.
24. Iaccarino G, Dolber PC, Lefkowitz RJ, Koch WJ. Beta-adrenergic receptor kinase-1 levels in the catecholamine-induced myocardial hypertrophy: regulation by beta- but not alpha1-adrenergic stimulation. *Hypertension.* 1999 Jan;33(1 Pt 2):396-401.
25. Iwai-Kanai E, Hasegawa K, Araki M, Kakita T, Morimoto T, Sasayama S. Alpha- and beta-adrenergic pathways differentially regulate cell type-specific apoptosis in rat cardiac myocytes. *Circulation.* 1999 Jul 20;100(3):305-11.
26. Jamali M, Rogerson PJ, Wilton S, Skerjanc IS. Nkx2-5 activity is essential for cardiomyogenesis. *J Biol Chem.* 2001 Nov 9;276(45):42252-8.

27. Karoor V, Shih M, Tholanikunnel B, Malbon CC. Regulating expression and function of G-protein linked receptors. *Prog Neurobiol.* 1996 Apr;48(6):555-68.
28. Kishimoto S, Maruo M, Ohse C, Yasuno H, Kimura H, Nagai T, Maeda T. The regeneration of the sympathetic catecholaminergic nerve fibers in the process of burn wound healing in guinea pigs. *J Invest Dermatol.* 1982 Sept;79(3):141-6.
29. Krishnamurthy P, Subramanian V, Singh M, Singh K. Beta1 integrins modulate beta-adrenergic receptor-stimulated cardiac myocyte apoptosis and myocardial remodeling. *Hypertension.* 2007 Apr;49(4):865-72.
30. Lee SH, Wolf PL, Escudero R, Deutsch R, Jamieson SW, Thistlethwaite PA. Early expression of angiogenesis factors in acute myocardial ischemia and infarction. *N Engl J Med.* 2000 Mar 2;342(9):626-33.
31. Lindsey ML, Gannon J, Aikawa M, Schoen FJ, Rabkin E, Lopresti-Morrow L, Crawford J, Black S, Libby P, Mitchell PG, Lee RT. Selective matrix metalloproteinase inhibition reduces left ventricular remodeling but does not inhibit angiogenesis after myocardial infarction. *Circulation.* 2002 Feb 12;105(6):753-8.

32. Lodish H, Berk A, Zipursky SL, Matsudaira P, Baltimore D, Darnell J. *Molecular Cell Biology*. 4th Edition. 2001.
33. Lui M, Warn JD, Fan Q, Smith PG. Relationships between nerves and myofibroblasts during cutaneous wound healing in the developing rat. *Cell Tissue Res*. 1999 Sep;297(3):423-33.
34. Matsuda H, Koyama H, Sato H, Sawada J, Itakura A, Tanaka A, Matsumoto M, Konno K, Ushio H, Matsuda K. Role of nerve growth factor in cutaneous wound healing : accelerating effects in normal and healing-impaired diabetic mice. *J Exp Med*. 1998 Feb 2;187(3):297-306.
35. Menon B, Singh M, Ross RS, Johnson JN, Singh K. beta-Adrenergic receptor-stimulated apoptosis in adult cardiac myocytes involves MMP-2-mediated disruption of beta1 integrin signaling and mitochondrial pathway. *Am J Physiol Cell Physiol*. 2006 Jan;290(1):C254-61.
36. Michalczyk K, Ziman M. Nestin structure and predicted function in cellular cytoskeletal organization. *Histol Histopathol*. 2005 Apr;20(2):665-71.
37. Mokry J, Pudil R, Ehrmann J, Cizkova D, Osterreicher J, Filip S, Kolar Z. Re-expression of nestin in the myocardium of postinfarcted patients. *Virchows Arch*. 2008 Jul;453(1):33-41.

38. Olivetti G, Capasso JM, Sonnenblick EH, Anversa P. Side-to-side slippage of myocytes participates in ventricular wall remodelling acutely after myocardial infarction in rats. *Circ Res.* 1990 Jul;67(1):23-34.
39. Perez E, Lopez-Briones LG, Gallar J, Belmonte C. Effects of chronic stimulation stimulation on corneal wound healing. *Invest Ophthalmol Vis Sci.* 1987 Feb;28(2):221-4.
40. Rohrer DK, Desai KH, Jasper JR, Stevens ME, Regula DJ, Barsh GS, Bernstein D, Kobilka BK. Targeted Disruption of the mouse beta1-adrenergic receptor: developmental and cardiovascular effects. *Proc Ntl Acad Sci U S A.* 1996 Jul 9;93(14):7375-80.
41. Rucker-Martin C, Milliez P, Tan S, Decrouy X, Recouvreur M, Vranckx R, Delcayre C, Renaud JF, Dunia I, Segretain D, Hatem SN. Chronic hemodynamic overload of the atria is an important factor for gap junction remodeling in human and rat hearts. *Cardiovasc Res.* 2006 Oct 1;72(1):69-79.
42. Sato M, Gong H, Terracciano CM, Ranu H, Harding SE. Loss of beta-adrenoceptor response in myocytes overexpressing the Na⁺/Ca²⁺-exchanger. *J Mol Cell Cardiol.* 2004 Jan;36(1):43-8.

43. Schwartz K, de la Bastie D, Bouveret P, Oliviero P, Alonso S, Buckingham M. Alpha-skeletal muscle actin mRNA's accumulate in hypertrophied adult rat hearts. *Circ Res.* 1986 Nov;59(5):551-5.
44. Scobioala S, Klocke R, Kuhlmann M, Tian W, Hasib L, Milting H, Koenig S, Stelljes M, El-Banayosy A, Tenderich G, Michel G, Breithardt G, Nikol S. Up-regulation of nestin in the infarcted myocardium potentially indicates differentiation of resident cardiac stem cells into various lineages including cardiomyocytes. *FASEB J.* 2008 Apr;22(4):1021-31.
45. Statistics Canada. *Health Reports*, Vol. 18, No. 3, August 2007.
46. Sutton MGSJ, Sharpe N. Left ventricular remodeling after myocardial infarction: pathophysiology and therapy. *Circulation.* 2000 Jun 27; 101(25):2981-8.
47. Swynghedauw B. Molecular mechanisms of myocardial remodeling. *Physiol Rev.* 1999 Jan;79(1):215-62.

48. Tepe NM, Lorenz JN, Yatani A, Dash R, Kranias EG, Dorn GW 2nd, Liggett SB. Altering the receptor-effector ratio by transgenic overexpression of type V adenylyl cyclase: enhanced basal catalytic activity and function without increased cardiomyocyte beta-adrenergic signalling. *Biochemistry*. 1999 Dec 14;38(50):16706-13.
49. Tomita Y, Matsumura K, Wakamatsu Y, Matsuzaki Y, Shibuya I, Kawaguchi H, Ieda M, Kanakubo S, Shimazaki T, Ogawa S, Osumi N, Okano H, Fukuda K. Cardiac neural crest cells contribute to the dominant multipotent stem cell in the mammalian heart. *J Cell Biol*. 2005 Sep 26;170(7):1135-46.
50. Vander A, Sherman JH, Luciano DS. *Human Physiology: The Mechanism of Body Function*. 8th Edition. 2001.
51. Voet D, Voet JG. *Biochemistry*. 3rd Edition. 2004.
52. Vracko R, Thorning D, Frederickson RG. Fate of nerve fibers in necrotic, healing, and healed rat myocardium. *Lab Invest*. 1990 Oct;63(4):490-501.
53. Wang B, Ansari R, Sun Y, Postlethwaite AE, Weber KT, Kiani MF. The scar neovasculature after myocardial infarction in rats. *Am J Physiol Heart Circ Physiol*. 2005 Jul;289(1):H108-13.

54. Wang W, Zhu W, Wang S, Yang D, Crow MT, Xiao RP, Cheng H. Sustained beta1-adrenergic stimulation modulates cardiac contractility by Ca²⁺/calmodulin kinase signaling pathway. *Circ Res.* 2004 Oct 15;95(8):798-806.
55. Wang Y, Ahmad N, Wani MA, Ashraf M. Hepatocyte growth factor prevents ventricular remodeling and dysfunction in mice via Akt pathway and angiogenesis. *J Mol Cell Cardiol.* 2004 Nov;37(5):1041-52.
56. Wurmser AE, Nakashima K, Summers RG, Toni N, D'Amour KA, Lie DC, Gage FH. Cell fusion-independent differentiation of neural stem cells to the endothelial lineage. *Nature.* 2004 Jul 15;430(6997):350-6.
57. Zhang LQ, Laato M. Innervation of normal and hypertrophic human scars and experimental wounds in the rat. *An Chir Gynaecol.* 2001;90 Suppl 215:29-32.
58. Zheng M, Han QD, Xiao RP. Distinct beta-adrenergic receptor subtype signaling in the heart and their pathophysiological relevance. *Acta Physiol Sinica.* 2004 Feb 25;56(1):1-15.

59. Zhou S, Chen LS, Miyauchi Y, Miyauchi M, Kar S, Kangavari S, Fishbein MC, Sharifi B, Chen PS. Mechanism of cardiac nerve sprouting in after myocardial infarction in dogs. *Circ Res.* 2004 Jul 9;95(1):76-83.
60. Zhu WZ, Zheng M, Koch WJ, Leftkowitz RJ, Kobilka BK, Xiao RP. Dual modulation of cell survival and cell death by beta(2)-adrenergic signaling in adult mouse cardiac myocytes. *Proc Ntl Acad Sci U S A.* 2001 Feb 13;98(4):1607-12.
61. Zhu W, Wang SQ, Chakir K, Yang D, Zhang T, Brown JH, Devic E, Kobilka BK, Cheng H, Xiao RP. Linkage of β_1 -adrenergic stimulation to apoptotic heart cell death through protein kinase A-independent activation of Ca^{2+} /calmodulin kinase II. *J Clin Invest.* 2003 Mar;111(5):617-25.